

TGF β targets the Hippo pathway scaffold RASSF1A to facilitate YAP/SMAD2 nuclear translocation.

Dafni-Eleftheria Pefani, Daniela Pankova, Aswin G. Abraham, Anna M. Grawenda, Nikola Vlahov, Simon Scrace and Eric O' Neill*.

CRUK/MRC Institute for Radiation Oncology, Department of Oncology, University of Oxford, OX3 7DQ, Oxford, UK.

*Corresponding author

Email: eric.oneill@oncology.ox.ac.uk

Tel: 0044 (0)1865 617321

Figures: 4

Supplemental Figures: 4

Supplemental Tables:2

Summary

Epigenetic inactivation of the Hippo pathway scaffold RASSF1A associates with poor prognosis in a wide range of sporadic human cancers. Loss of expression reduces tumor suppressor activity and promotes genomic instability, but how this pleiotropic biomarker is regulated at the protein level is unknown. Here we show that TGF β is the physiological signal that stimulates RASSF1A degradation by the ubiquitin-proteasome pathway. In response to TGF β , RASSF1A is recruited to TGF β Receptor I and is targeted for degradation by the co-recruited E3 ubiquitin ligase, ITCH. RASSF1A degradation is necessary to permit Hippo pathway effector YAP1 association with SMADs and subsequent nuclear translocation of receptor activated SMAD2. We find that RASSF1A expression regulates TGF β induced YAP1/SMAD2 interaction, leads to SMAD2 cytoplasmic retention and inefficient transcription of TGF β targets genes. Moreover, RASSF1A limits TGF β induced invasion, offering a new framework on how RASSF1A affects YAP1 transcriptional output and elicits its tumor suppressive function.

Introduction

Epigenetic inactivation of RASSF1A correlates with poor clinicopathological characteristics in nearly all solid tumors (Grawenda and O'Neill, 2015). In addition to epigenetic inactivation, germline alteration of RASSF1A is also linked with cancer onset and poor cancer prognosis, mainly through its role in regulating the Hippo tumor suppressor pathway (Pefani et al., 2014; Pefani and O'Neill, 2016) and the transcription co-factor YAP1 (Yee et al., 2012). However, despite the widespread clinical evidence, little is known about RASSF1A regulation by environmental cues.

Transforming growth factor- β (TGF β) acts in both an autocrine and paracrine manner to regulate cell growth, differentiation and migration (Bierie and Moses, 2006). TGF β plays a crucial role in tumor microenvironment, but a dichotomy exists as there are well described roles for the TGF β pathway promoting both tumor suppression, during tumor initiation, and tumor progression, during later stage disease (Massague, 2008). In response to TGF β mediated dimerization of TGF β RI and II, receptor-regulated SMADs (SMAD2/3) are phosphorylated, complex with SMAD4, and translocate to the nucleus to engage DNA-binding partners and transcriptional co-activators (Feng and Derynck, 2005). The shuttling of SMAD complexes between the cytoplasm and the nucleus is carefully regulated and it has been proposed that nuclear retention correlates with the strength of the signal (Schmierer et al., 2008). Importin/Exportin and nucleoporin dependent mechanisms have been shown to mediate SMAD nuclear accumulation (Kurisaki et al., 2001; Xu et al., 2002). Moreover, SMAD2/3 interaction with YAP/TAZ Hippo pathway effectors plays a central role in SMAD nuclear-cytoplasmic shuttling. In the absence of YAP/TAZ, SMADs fail to accumulate in the nucleus and TGF β mediated transcription is disabled (Varelas et al., 2008). Moreover, the Hippo pathway couples cell density with TGF β activity. Varelas *et al.* previously showed that in polarized epithelial cells retention of YAP1 in the cytoplasm abrogated SMAD nuclear translocation and TGF β transcription (Varelas et al., 2008; Varelas et al., 2010). However, it still remains unknown how YAP/SMAD2/3 interaction is regulated in tumor cells once epithelial polarity is lost, e.g. in metastatic tumors.

YAP/TAZ oncogenic transcription is mainly described to be promoted through binding to TEAD transcription factors (Zhao et al., 2008). YAP1/SMAD transcriptional

complexes contribute to oncogenic phenotypes in combination with TEAD, suggesting that YAP1 promotes and maintains the tumorigenic activity of the TGF β pathway (Fujii et al., 2012; Hiemer et al., 2014). To restrict cell growth or respond to stress, the Hippo pathway both negatively regulates TEAD and increases YAP affinity for p73 to promote apoptosis (Strano et al., 2001). RASSF1A is a key mediator of Hippo pathway activity that mediates this switch to regulate oncogenic versus tumor suppressive activity via differential transcription factor binding of YAP (Ahn et al., 2013; Hamilton et al., 2009; van der Weyden et al., 2012).

In this study, we employed a bioinformatics analysis of tumor cohorts looking for key pathways perturbed by loss of RASSF1A and identified TGF β signaling to be amongst the most consistent tumor related pathways altered. Importantly, we find that RASSF1A recruitment to active TGF β RI results in endogenous protein degradation by ITCH E3 ligase. We show that RASSF1A degradation allows YAP1 to interact with SMAD2, promoting SMAD2 nuclear translocation and transcriptional activation of TGF β responsive targets that results in cellular invasion.

Results

RASSF1A is degraded in response to TGF β signaling.

Originally identified as a tumor suppressor event in lung and breast cancers, epigenetic silencing of the *RASSF1A* gene has been widely associated with poor patient outcome. To uncover the signaling pathways which are perturbed by *RASSF1A* methylation, we undertook an unbiased screening approach of the two tumor types where clinical evidence is most robust, non-small cell lung cancer (specifically adenocarcinoma) and invasive breast cancer. We employed both RNAseq and HM450K Illumina methylation chip data available from The Cancer Genome Atlas (TCGA) to access the effects of RASSF1A levels in cohorts as correlations between genomic gene methylation and gene expression can vary considerably (Pastuszak-Lewandoska et al., 2015; van Eijk et al., 2012). We performed a Gene Set Enrichment Analysis (GSEA) for oncogenic signatures in tumors with positive or negative RASSF1A mRNA expression (analysis 1) or tumors displaying high vs low levels of *RASSF1A* gene methylation (bottom100 vs top100, analysis 2-Top 50 hits of each analysis given in

Table S1 and S2). The combined analysis identified 146 signatures significantly enriched across the two distinct analyses and two tumor datasets which could be grouped into 10 functional groups spanning roles in immune signaling, development, genome maintenance and cancer (Figure 1A). To identify the most relevant signatures associated with the poor prognostic phenotype of RASSF1A loss in cancer, we next cross-validated the signatures that were identified from both analysis 1 (RASSF1A mRNA) and analysis 2 (RASSF1A methylation) of the TCGA lung adenocarcinoma and invasive breast cancer cohorts. Only 21 specific gene signatures were found in both mRNA and methylation analyses in lung and 22 in breast (including the YAP/TAZ Hippo pathway signature) (Figure 1B, Tables S1 & S2). We next looked for overlap between the two tumor types and identified 8 signatures that were significantly altered in both tumor types (Figure 1B). Interestingly, the TGF β gene set showed significance across all four analyses where RASSF1A gene expression is affected ($p=0.0001$). We have recently demonstrated that loss of RASSF1A promotes epithelial mesenchymal transition, a tumor progression phenotype also promoted by TGF β signaling (Vlahov et al., 2015). As TGF β signaling had also been linked to RASSF1A stability (Bhaskaran and Souchelnytskyi, 2008) we reasoned that TGF β may regulate endogenous RASSF1A and the absence of expression in methylated tumors may affect TGF β transcriptional output. To determine whether RASSF1A is responsive to ligand induced activation of the receptor, we first screened lung cancer cell lines from the NCI-60 panel for endogenous expression of RASSF1A (Figure S1A). Only HOP92 cells demonstrated appreciable protein levels compared to HeLa cells, which were significantly reduced upon exposure to TGF β , indicating that RASSF1A may be targeted for degradation (Figure 1C). To rule out TGF β mediated epigenetic silencing (Papageorgis et al., 2010) or SMAD transcriptional repression, we next utilized U2OS and H1299 derivative cell lines which had previously been engineered to express RASSF1A under a doxycycline inducible promoter similar to endogenous protein levels (Figure S1B). In both cell lines, RASSF1A reduction was evident after 2 hours of exposure to TGF β treatment (Figure 1D and S1C). Moreover, in the presence of the proteasome inhibitor MG132, RASSF1A protein was stabilized indicating that TGF β dependent regulation of RASSF1A is proteasome mediated (Figure 1E and 1F). Moreover, addition of the TGF β RI Kinase inhibitor II (E-616451) could maintain RASSF1A stability (Figure 1E).

To verify that TGF β -mediated downregulation of RASSF1A is due to protein degradation we performed an *in vivo* ubiquitination assay and observed increased mono- and poly-ubiquitination after a 2-hour treatment with TGF β (Figure 1G). Background ubiquitination could be partially attributed to endogenous paracrine TGF β signaling (Figure S1D), and TGF β - independent RASSF1A ubiquitination (Jiang et al., 2011; Song et al., 2008). We next utilized NBE-1 (Normal Bronchial Epithelial cells) and MCF10A (mammary epithelial cells) to assess RASSF1A levels after treatment with TGF β in primary cell lines. As in cancer cells, treating primary cell lines with TGF β resulted in downregulation of RASSF1A protein levels (Figure 1H). The above data outlines that the widespread tumor suppressor, RASSF1A is downregulated by a key tumor microenvironmental stimulus, TGF β .

RASSF1A is targeted by ITCH E3 ligase via recruitment to TGF β RI.

Previous studies have shown RASSF1A recruitment to death receptor complexes promotes cell death and inhibits tumor formation (Foley et al., 2008), therefore we reasoned that TGF β may trigger degradation of RASSF1A following direct association with TGF β receptors. In HOP92 cells endogenous RASSF1A is associated with internal microtubule structures in control cells (Figure 2A and S1E). Upon TGF β treatment, RASSF1A signal is significantly decreased however the remaining RASSF1A was found accumulated at the membrane (Figure 2A and S1E). We also detected a limited association of FLAG-RASSF1A with endogenous TGF β RI and II in the absence of TGF β and a clear stimulation of RASSF1A/ TGF β RI interaction in TGF β treated cells (Figure 2B and S1F). To further characterize TGF β RI-RASSF1A interaction we used a series of RASSF1A truncated mutants to determine the domain responsible for the interaction. As shown in Figure 2C, full length RASSF1A (1-340) associates with the receptor but derivatives lacking the N-Terminal C1 domain failed to do so, suggesting this domain is necessary for the binding to the receptor. C1 domains are known to mediate membrane targeting (Colon-Gonzalez and Kazanietz, 2006) and to be necessary for RASSF1A interaction with the TNF- α receptor (Foley et al., 2008).

We next questioned the identity of the E3-ligase responsible for RASSF1A degradation after recruitment to the TGF β RI. ITCH is an E3 ligase known to interact with TGF β RI

and ubiquitinate SMAD2 to promote SMAD2 association with TGF β RI and subsequent phosphorylation to activate the pathway ((Bai et al., 2004) and Figure S1G) and has been shown to regulate Hippo pathway components including the RASSF1 homolog, RASSF5 (Salah et al., 2011; Suryaraja et al., 2013). Interestingly, ITCH was identified in FLAG-RASSF1A immunoprecipitates (Figure 2D). To test potential RASSF1A regulation by ITCH, we examined the stability of both endogenous and stably expressed (promoter independent) RASSF1A in response to TGF β stimulation after siRNA mediated depletion of ITCH. As shown in Figure 2E, S1H and S1I, ITCH knockdown rescues the reduction of RASSF1A upon TGF β treatment in HOP92, EKVX and U2OS^{TetON-RASSF1A} cells compared to controls. We also show that RASSF1A is a direct target of ITCH using an *in vitro* ubiquitination assay (Figure S1J) and that ITCH is required for efficient targeting of RASSF1A in cells exposed to TGF β (Figure 2F). Moreover, re-expression of wild type (ITCH-WT) but not of a catalytic inactive mutant (ITCH-CA) indicates that ITCH catalytic activity is necessary for RASSF1A degradation in response to TGF β stimulation (Figure 2G). Interestingly, we observe an inverse correlation of ITCH levels and RASSF1A accumulation amongst the NCI-60 panel (Figure S1K). Low levels of ITCH in HOP92 cells could contribute to RASSF1A accumulation in addition to low promoter methylation. The above data show that ITCH E3-ligase regulates RASSF1A TGF β -dependent degradation, while residual RASSF1A ubiquitination in ITCH siRNA treated cells implies that additional ligases may compensate for the loss of ITCH.

RASSF1A restrains nuclear localization of SMAD2 via regulation of YAP1 binding.

To determine whether RASSF1A degradation has any consequence to TGF β signaling, we first considered the previously reported links between the RASSF1A/Hippo pathway effector YAP1 and the TGF β effector SMADs. In response to TGF β signaling, YAP1, and close homolog TAZ (WWTR1), interact with SMAD2/3 to promote their nuclear translocation (Varelas et al., 2008; Varelas et al., 2010). RASSF1A is a core component of the Hippo pathway that regulates YAP1 interaction with transcription factors (Ahn et al., 2013; Hamilton et al., 2009; van der Weyden et al., 2012). Since TGF β stimulation resulted in RASSF1A downregulation, we questioned whether YAP1/TAZ interaction with SMAD2 may be affected. As previously shown, TGF β

treatment stimulates YAP1/SMAD2 binding, however, this is significantly retarded upon RASSF1A overexpression and switching of YAP1 binding to the alternative tumor suppressor partner p73 is favored (Figure 3A). Despite less efficient YAP1/p73 complex formation in TGF β treated compared to untreated cells due to reduced RASSF1A levels in the presence of the ligand, there is still a functional increase in YAP1/p73 and induction of the p73 target gene product, PUMA (Figure S2A). TEAD transcription factors form trimeric YAP-TEAD-SMAD complexes that coordinate oncogenic transcriptional events in a concerted manner (Fujii et al., 2012; Hiemer et al., 2014). RASSF1A has been shown to promote YAP1/p73 interaction in expense of YAP1/TEAD (van der Weyden et al., 2012). Induction of RASSF1A expression in U2OS^{TetON-RASSF1A} cells also resulted in decreased YAP1/TEAD2 interaction in the presence of the ligand, further validating RASSF1A as a regulator of transcriptional choices in response to TGF β signaling (Figure S2B). Interestingly, RASSF1A overexpression did not affect TAZ interaction with SMAD2 indicating a potential specificity for the regulation of YAP1/SMAD2 by RASSF1A (Figure S2C). As the interaction between YAP1 and SMAD2 is required for nuclear translocation upon TGF β stimulation, we next monitored the effect of RASSF1A on nuclear SMAD2. RASSF1A expression resulted in less efficient nuclear translocation and increased cytoplasmic retention of SMAD2 keeping in line with reduced YAP1 association (Figure 3B and 3C, Figure S2D and S2E). A proportion of SMAD2 is retained in the nuclear fraction under these conditions, most likely due to TAZ dependent nuclear shuttling. In agreement with preventing nuclear translocation, RASSF1A overexpression also inhibited TGF β -dependent induction of the SMAD2 transcriptional targets *Smad7*, *PAI-1* and *CTGF* (Nakao et al., 1997; Westerhausen et al., 1991; Xie et al., 2005) (Figure 3D). Thus, these data suggests that RASSF1A is a negative regulator of TGF β dependent transcription via limiting SMAD2 nuclear translocation and subsequent transcription.

Reduction of RASSF1A levels in HOP92 cells, using two independent siRNAs, increased YAP1/SMAD2 interaction upon TGF β addition (Figure 3E), validating that the rate limiting function of RASSF1A is in YAP1 partner selection. To further study the effect of RASSF1A ablation in SMAD2 localization we used genetically ablated *Rassf1A*^{-/-} Mouse Embryonic Fibroblasts (MEFs). Upon TGF β stimulation, SMAD2 nuclear accumulation is enhanced in the absence of RASSF1A compared to control conditions

(Figure 3F and 3H, Figure S2F). Most strikingly, significant levels of nuclear SMAD2 are evident in the absence of stimulus in *Rassf1A*^{-/-} MEFs (Figure 3G). We confirmed the increased levels of TGFβ stimulated nuclear SMAD2 by depleting RASSF1A in HOP92 cells (Figure S2G). In agreement, the expression of the SMAD2 transcriptional targets *Smad7*, *PAI-1* and *CTGF* were elevated in HOP92 (lung cancer), MCF10A and NBE-1 after RASSF1A depletion (Figure 3I and S3A and S3B). *CTGF* induction did not show any significant increase in the absence of RASSF1A in NBE-1 cells indicating potential additional regulation of *CTGF* expression in this cell line.

YAP1 also interacts with SMAD1 in response to the TGFβ superfamily signaling peptide, BMP4. YAP1 binding to SMAD1 enhances its transcriptional activity via stimulation of SMAD1 linker phosphorylation by CDK8/9 (Alarcon et al., 2009). RASSF1A overexpression has a similar effect on YAP1 binding to SMAD1 as found for SMAD2, resulting in decreased SMAD1/YAP1 complexes response to BMP4 signaling (Figure S3C). Moreover, RASSF1A overexpression significantly affected the BMP transcriptional response leading to decreased activation of the *Id1*, *Id2* and *Id3* expression in mESCs (Figure S3D), showing that RASSF1A may affect transcriptional output of the TGFβ superfamily by regulating YAP1.

RASSF1A suppresses TGFβ induced invasion.

RASSF1A methylation has been correlated with increased invasiveness and metastasis in cancer patients (Bilgrami et al., 2014; Fackler et al., 2003; Korah et al., 2013). TGFβ signaling is known to promote Epithelial to Mesenchymal Transition (EMT) that significantly contributes to tumor invasion and metastasis (Xu et al., 2009). In order to assess whether TGFβ induced invasion requires RASSF1A degradation we employed a transwell invasion assay, and found that upon induction of RASSF1A expression in U2OS^{TetON-RASSF1A}, TGFβ dependent invasion was significantly impaired (Figure 4A). In agreement with single cell approaches, relative spheroid invasion in 3D collagen matrix (as determined by the extent of spike-like protrusions) showed that RASSF1A overexpression results in a statistically significant reduction of invasiveness compared to non-induced cells (Figure 4B). Similar results were observed after induction of RASSF1A in H1299^{TetON-RASSF1A} cells and expression in NCI-H460 cells (Figures S4A, B).

Depletion of ITCH from U2OS^{TetON-RASSF1A} resulted in decreased TGF β mediated invasion, compatible with a role for ITCH as a positive regulator of TGF β signaling via promoting SMAD2 phosphorylation independently of RASSF1A regulation, and did not further affect RASSF1A dependent reduction of invasiveness (Figure S4C) (Bai et al., 2004). To confirm that RASSF1A regulates TGF β mediated invasion through SMADs we co-depleted RASSF1A and SMAD2 or SMAD3 from HOP92 cells and addressed invasiveness compared to siRASSF1A treated cells (Figure S4D). SMAD2 deletion appeared to have a more robust effect in eliminating siRASSF1A induced invasion in response to TGF β compared to SMAD3, potentially due to different target regulation or less efficient SMAD3 knock down ((Brown et al., 2007) Figure S4D)). The above results indicate that RASSF1A restricts invasion by limiting TGF β mediated transcription, and explains specific correlation of RASSF1A methylation with invasive and metastatic tumors in the clinic

Discussion

Both epigenetic regulation (promoter methylation) and genetic changes (somatic mutations or SNPs) in RASSF1A are correlated with cancer susceptibility and have cancer prognostic significance (Grawenda and O'Neill, 2015). Although RASSF1A protein levels have been proposed to fluctuate during cell cycle (Jiang et al., 2011; Song et al., 2008), a clear connection with a physiological signal that modulates RASSF1A protein levels has been lacking. Here we identify TGF β as a tumor microenvironmental signal that promotes RASSF1A degradation, resulting in an altered TGF β transcriptional program in lung and breast cancer patients.

We found that RASSF1A interaction with the ligand-bound TGF β receptor tetramer is mediated by the N-terminal C1 domain, often found mutated in tumors that retain expression (van der Weyden and Adams, 2007). Furthermore, the ITCH E3 ligase responsible for degradation of RASSF1A is also known to localize at TGF β RI in response to TGF β stimulation where it catalyzes SMAD2 ubiquitination to enhance SMAD2 phosphorylation and subsequent TGF β transcriptional activity (Bai et al., 2004). This implies that ITCH may facilitate TGF β signaling by both upregulating SMAD2 phosphorylation and promoting association with YAP1.

RASSF1A activation stimulates the proapoptotic activity of the Hippo pathway by promoting YAP1 binding to p73 (Hamilton et al., 2009) while limiting the binding to oncogenic TEAD factors (van der Weyden et al., 2012) that complex with SMAD2 to elicit TGF β oncogenic activity (Hiemer et al., 2014). Similarly, we find that when RASSF1A is overexpressed, we observe limited SMAD2 binding to YAP1 and increased association with p73, in contrast ablation of RASSF1A favors YAP1/SMAD interaction. YAP/TAZ binding to SMAD2 is crucial for nuclear translocation and an efficient TGF β transcriptional response (Varelas et al., 2008; Varelas et al., 2010). Previous studies also demonstrated that activation of the Hippo pathway by the Crumbs polarity complex in high-density monolayers, leads to Hippo dependent inhibition of TGF β transcription due to cytoplasmic retention of YAP1/SMAD2 (Varelas et al., 2010). In agreement, we find that Hippo pathway activation, here by RASSF1A, negatively regulates the remaining nuclear YAP1/SMAD2 fraction leading to limited TGF β transcriptional activation. Interestingly we did not observe significant changes in TAZ binding to SMAD2 upon RASSF1A overexpression, highlighting a physiological separation of YAP1 and TAZ regulation. Therefore we conclude that TGF β mediated RASSF1A degradation aims to allow efficient SMAD2 nuclear accumulation and an efficient transcriptional response (Figure 4D).

TGF β signaling promotes EMT and cancer invasion during cancer progression (Padua and Massague, 2009), while nuclear TAZ/YAP are also associated with promoting EMT (Chan et al., 2008; Overholtzer et al., 2006). More recently it was shown that YAP, SMAD2/3 and TEAD converge to regulate a TGF β induced transcriptional programme that induces migration and invasion in breast cancers (Hiemer et al., 2014). Similarly, YAP/TEAD/Smad3/p300 complex was found to drive *CTGF* expression in malignant mesothelioma resulting in increased tumor growth (Fujii et al., 2012). We recently showed that RASSF1A also inhibits YAP1 mediated cell invasion in a SRC kinase dependent manner (Vlahov et al., 2015), which is in line with clinical correlations with increased invasiveness and metastasis in *RASSF1* methylated tumors (Bilgrami et al., 2014; Fackler et al., 2003; Korah et al., 2013). Here we provide evidence that RASSF1A eliminates TGF β induced invasion in keeping with increasing reports supporting a role for RASSF1A in invasion (Dubois et al., 2016; Lee et al., 2016), offering a further mechanistic insight on how RASSF1A elicits its tumor suppressive function (Figure 4D).

Aberrant TGF β signaling activity regulates tumor progression and these effects may be tumor suppressing or tumor promoting depending on the somatic context (David et al., 2016). In RASSF1A methylated cancers, tumor cells appear to mimic a TGF β active state that leads to increased oncogenic YAP1/SMAD2 nuclear accumulation, resulting in aggressive malignant phenotypes. Therefore, we propose a mechanistic explanation for the role of RASSF1A in tumor suppression and an epigenetic event influencing TGF β tumor suppressive versus oncogenic signaling.

Experimental procedures

Methylation, Gene expression profiling and GSEA

Data sets for the meta-analysis in Figure 1A and B and Tables S1 and S2 are accessible from The Cancer Genome Atlas database (TCGA; <http://gdac.broadinstitute.org>). LUAD represents Lung Adenocarcinoma subgroup of non-small cell lung cancer encompassing n=515 patients with available RNAseq data (2015_04_02 stddata). BRCA represents samples from all invasive breast cancer encompassing n=1048 patients with available RNAseq (2014_06_14 stddata). For TCGA data methylation values were attained from the Illumina HumanMethylation450 Bead Chip array (HM450K, data level 3) for the RASSF1 gene to rank tumours from 0.0 (lowest) to 1.0 (maximal), RASSF1A expression data was performed by taking RNASeqV12 RSEM isoforms level3 uc003dae.1 isoform result for individual samples. RASSF1A high and low methylation grouping were selected by ranking levels of RASSF1A average promoter methylation and partitioning on the top 100 and bottom 100 values. RASSF1A positive mRNA expression grouping was selected based on raw count RNAseq values above zero, whereby RASSF1A negative grouping consisted of all samples with a raw count equal to zero. Gene Set Enrichment Analysis GSEA with RNASeqV12 RSEM normalised genes data level3 was used to assess enrichment of Oncogenic signatures (c6.all.v4.0symbols.gmt gene sets database) in each group and the table of results is listed in Tables S1 and S2 (<http://www.broadinstitute.org/gsea/index.jsp>). Overlaps between groups were limited to exact signature matches and binomial correlation used to determine the statistical significance of signature appearing in all four groups.

Detailed experimental procedures, cell lines, treatments, details on siRNA oligonucleotide sequences used are available on the Supplemental Experimental Procedures.

References

- Ahn, E.Y., Kim, J.S., Kim, G.J., and Park, Y.N. (2013). RASSF1A-mediated regulation of AREG via the Hippo pathway in hepatocellular carcinoma. *Molecular cancer research : MCR* *11*, 748-758.
- Alarcon, C., Zaromytidou, A.I., Xi, Q., Gao, S., Yu, J., Fujisawa, S., Barlas, A., Miller, A.N., Manova-Todorova, K., Macias, M.J., *et al.* (2009). Nuclear CDKs drive Smad transcriptional activation and turnover in BMP and TGF-beta pathways. *Cell* *139*, 757-769.
- Bai, Y., Yang, C., Hu, K., Elly, C., and Liu, Y.C. (2004). Itch E3 ligase-mediated regulation of TGF-beta signaling by modulating smad2 phosphorylation. *Molecular cell* *15*, 825-831.
- Bhaskaran, N., and Souhelnytskyi, S. (2008). Systemic analysis of TGFbeta proteomics revealed involvement of Plag1/CNK1/RASSF1A/Src network in TGFbeta1-dependent activation of Erk1/2 and cell proliferation. *Proteomics* *8*, 4507-4520.
- Bierie, B., and Moses, H.L. (2006). Tumour microenvironment: TGFbeta: the molecular Jekyll and Hyde of cancer. *Nat Rev Cancer* *6*, 506-520.
- Bilgrami, S.M., Qureshi, S.A., Pervez, S., and Abbas, F. (2014). Promoter hypermethylation of tumor suppressor genes correlates with tumor grade and invasiveness in patients with urothelial bladder cancer. *SpringerPlus* *3*, 178.
- Brown, K.A., Pietenpol, J.A., and Moses, H.L. (2007). A tale of two proteins: differential roles and regulation of Smad2 and Smad3 in TGF-beta signaling. *Journal of cellular biochemistry* *101*, 9-33.
- Chan, S.W., Lim, C.J., Guo, K., Ng, C.P., Lee, I., Hunziker, W., Zeng, Q., and Hong, W. (2008). A role for TAZ in migration, invasion, and tumorigenesis of breast cancer cells. *Cancer Res* *68*, 2592-2598.
- Colon-Gonzalez, F., and Kazanietz, M.G. (2006). C1 domains exposed: from diacylglycerol binding to protein-protein interactions. *Biochimica et biophysica acta* *1761*, 827-837.
- David, C.J., Huang, Y.H., Chen, M., Su, J., Zou, Y., Bardeesy, N., Iacobuzio-Donahue, C.A., and Massague, J. (2016). TGF-beta Tumor Suppression through a Lethal EMT. *Cell* *164*, 1015-1030.
- Dubois, F., Keller, M., Calvayrac, O., Soncin, F., Hoa, L., Hergovich, A., Parrini, M.C., Mazieres, J., Vaisse-Lesteven, M., Camonis, J., *et al.* (2016). RASSF1A suppresses the invasion and metastatic potential of human non-small cell lung cancer cells by inhibiting YAP activation through the GEF-H1/RhoB pathway. *Cancer Res.*
- Fackler, M.J., McVeigh, M., Evron, E., Garrett, E., Mehrotra, J., Polyak, K., Sukumar, S., and Argani, P. (2003). DNA methylation of RASSF1A, HIN-1, RAR-beta, Cyclin D2 and Twist in in situ and invasive lobular breast carcinoma. *International journal of cancer. Journal international du cancer* *107*, 970-975.
- Feng, X.H., and Derynck, R. (2005). Specificity and versatility in tgf-beta signaling through Smads. *Annual review of cell and developmental biology* *21*, 659-693.

Foley, C.J., Freedman, H., Choo, S.L., Onyskiw, C., Fu, N.Y., Yu, V.C., Tuszynski, J., Pratt, J.C., and Baksh, S. (2008). Dynamics of RASSF1A/MOAP-1 association with death receptors. *Molecular and cellular biology* 28, 4520-4535.

Fujii, M., Toyoda, T., Nakanishi, H., Yatabe, Y., Sato, A., Matsudaira, Y., Ito, H., Murakami, H., Kondo, Y., Kondo, E., *et al.* (2012). TGF-beta synergizes with defects in the Hippo pathway to stimulate human malignant mesothelioma growth. *The Journal of experimental medicine* 209, 479-494.

Grawenda, A.M., and O'Neill, E. (2015). Clinical utility of RASSF1A methylation in human malignancies. *Br J Cancer* 113, 372-381.

Hamilton, G., Yee, K.S., Scrace, S., and O'Neill, E. (2009). ATM regulates a RASSF1A-dependent DNA damage response. *Curr Biol* 19, 2020-2025.

Hiemer, S.E., Szymaniak, A.D., and Varelas, X. (2014). The transcriptional regulators TAZ and YAP direct transforming growth factor beta-induced tumorigenic phenotypes in breast cancer cells. *The Journal of biological chemistry* 289, 13461-13474.

Jiang, L., Rong, R., Sheikh, M.S., and Huang, Y. (2011). Cullin-4A.DNA damage-binding protein 1 E3 ligase complex targets tumor suppressor RASSF1A for degradation during mitosis. *The Journal of biological chemistry* 286, 6971-6978.

Korah, R., Healy, J.M., Kunstman, J.W., Fonseca, A.L., Ameri, A.H., Prasad, M.L., and Carling, T. (2013). Epigenetic silencing of RASSF1A deregulates cytoskeleton and promotes malignant behavior of adrenocortical carcinoma. *Molecular cancer* 12, 87.

Kurisaki, A., Kose, S., Yoneda, Y., Heldin, C.H., and Moustakas, A. (2001). Transforming growth factor-beta induces nuclear import of Smad3 in an importin-beta1 and Ran-dependent manner. *Molecular biology of the cell* 12, 1079-1091.

Lee, M.G., Jeong, S.I., Ko, K.P., Park, S.K., Ryu, B.K., Kim, I.Y., Kim, J.K., and Chi, S.G. (2016). RASSF1A directly antagonizes RhoA activity through the assembly of a Smurf1-mediated destruction complex to suppress tumorigenesis. *Cancer Res.*

Massague, J. (2008). TGFbeta in Cancer. *Cell* 134, 215-230.

Nakao, A., Afrakhte, M., Moren, A., Nakayama, T., Christian, J.L., Heuchel, R., Itoh, S., Kawabata, M., Heldin, N.E., Heldin, C.H., *et al.* (1997). Identification of Smad7, a TGFbeta-inducible antagonist of TGF-beta signalling. *Nature* 389, 631-635.

Overholtzer, M., Zhang, J., Smolen, G.A., Muir, B., Li, W., Sgroi, D.C., Deng, C.X., Brugge, J.S., and Haber, D.A. (2006). Transforming properties of YAP, a candidate oncogene on the chromosome 11q22 amplicon. *Proceedings of the National Academy of Sciences of the United States of America* 103, 12405-12410.

Padua, D., and Massague, J. (2009). Roles of TGFbeta in metastasis. *Cell research* 19, 89-102.

Papageorgis, P., Lambert, A.W., Ozturk, S., Gao, F., Pan, H., Manne, U., Alekseyev, Y.O., Thiagalingam, A., Abdolmaleky, H.M., Lenburg, M., *et al.* (2010). Smad signaling is required to maintain epigenetic silencing during breast cancer progression. *Cancer Res* 70, 968-978.

Pastuszak-Lewandoska, D., Kordiak, J., Migdalska-Sek, M., Czarnecka, K.H., Antczak, A., Gorski, P., Nawrot, E., Kiszalkiewicz, J.M., Domanska, D., and Brzezianska-Lasota, E. (2015). Quantitative analysis of mRNA expression levels and DNA methylation profiles of three neighboring genes: FUS1, NPRL2/G21 and RASSF1A in non-small cell lung cancer patients. *Respiratory research* 16, 76.

Pefani, D.E., Latusek, R., Pires, I., Grawenda, A.M., Yee, K.S., Hamilton, G., van der Weyden, L., Esashi, F., Hammond, E.M., and O'Neill, E. (2014). RASSF1A-LATS1

signalling stabilizes replication forks by restricting CDK2-mediated phosphorylation of BRCA2. *Nat Cell Biol* 16, 962-971.

Pefani, D.E., and O'Neill, E. (2016). Hippo pathway and protection of genome stability in response to DNA damage. *The FEBS journal* 283, 1392-1403.

Salah, Z., Melino, G., and Aqeilan, R.I. (2011). Negative regulation of the Hippo pathway by E3 ubiquitin ligase ITCH is sufficient to promote tumorigenicity. *Cancer Res* 71, 2010-2020.

Schmierer, B., Tournier, A.L., Bates, P.A., and Hill, C.S. (2008). Mathematical modeling identifies Smad nucleocytoplasmic shuttling as a dynamic signal-interpreting system. *Proceedings of the National Academy of Sciences of the United States of America* 105, 6608-6613.

Song, M.S., Song, S.J., Kim, S.J., Nakayama, K., Nakayama, K.I., and Lim, D.S. (2008). Skp2 regulates the antiproliferative function of the tumor suppressor RASSF1A via ubiquitin-mediated degradation at the G1-S transition. *Oncogene* 27, 3176-3185.

Strano, S., Munarriz, E., Rossi, M., Castagnoli, L., Shaul, Y., Sacchi, A., Oren, M., Sudol, M., Cesareni, G., and Blandino, G. (2001). Physical interaction with Yes-associated protein enhances p73 transcriptional activity. *The Journal of biological chemistry* 276, 15164-15173.

Suryaraja, R., Anitha, M., Anbarasu, K., Kumari, G., and Mahalingam, S. (2013). The E3 ubiquitin ligase Itch regulates tumor suppressor protein RASSF5/NORE1 stability in an acetylation-dependent manner. *Cell death & disease* 4, e565.

van der Weyden, L., and Adams, D.J. (2007). The Ras-association domain family (RASSF) members and their role in human tumorigenesis. *Biochimica et biophysica acta* 1776, 58-85.

van der Weyden, L., Papaspyropoulos, A., Poulogiannis, G., Rust, A.G., Rashid, M., Adams, D.J., Arends, M.J., and O'Neill, E. (2012). Loss of RASSF1A synergizes with deregulated RUNX2 signaling in tumorigenesis. *Cancer Res* 72, 3817-3827.

van Eijk, K.R., de Jong, S., Boks, M.P., Langeveld, T., Colas, F., Veldink, J.H., de Kovel, C.G., Janson, E., Strengman, E., Langfelder, P., *et al.* (2012). Genetic analysis of DNA methylation and gene expression levels in whole blood of healthy human subjects. *BMC genomics* 13, 636.

Varelas, X., Sakuma, R., Samavarchi-Tehrani, P., Peerani, R., Rao, B.M., Dembowy, J., Yaffe, M.B., Zandstra, P.W., and Wrana, J.L. (2008). TAZ controls Smad nucleocytoplasmic shuttling and regulates human embryonic stem-cell self-renewal. *Nat Cell Biol* 10, 837-848.

Varelas, X., Samavarchi-Tehrani, P., Narimatsu, M., Weiss, A., Cockburn, K., Larsen, B.G., Rossant, J., and Wrana, J.L. (2010). The Crumbs complex couples cell density sensing to Hippo-dependent control of the TGF-beta-SMAD pathway. *Developmental cell* 19, 831-844.

Vlahov, N., Scrace, S., Soto, M.S., Grawenda, A.M., Bradley, L., Pankova, D., Papaspyropoulos, A., Yee, K.S., Buffa, F., Goding, C.R., *et al.* (2015). Alternate RASSF1 Transcripts Control SRC Activity, E-Cadherin Contacts, and YAP-Mediated Invasion. *Current biology : CB* 25, 3019-3034.

Westerhausen, D.R., Jr., Hopkins, W.E., and Billadello, J.J. (1991). Multiple transforming growth factor-beta-inducible elements regulate expression of the plasminogen activator inhibitor type-1 gene in Hep G2 cells. *The Journal of biological chemistry* 266, 1092-1100.

Xie, S., Sukkar, M.B., Issa, R., Oltmanns, U., Nicholson, A.G., and Chung, K.F. (2005). Regulation of TGF-beta 1-induced connective tissue growth factor expression in airway smooth muscle cells. *American journal of physiology. Lung cellular and molecular physiology* 288, L68-76.

Xu, J., Lamouille, S., and Derynck, R. (2009). TGF-beta-induced epithelial to mesenchymal transition. *Cell research* 19, 156-172.

Xu, L., Kang, Y., Col, S., and Massague, J. (2002). Smad2 nucleocytoplasmic shuttling by nucleoporins CAN/Nup214 and Nup153 feeds TGFbeta signaling complexes in the cytoplasm and nucleus. *Molecular cell* 10, 271-282.

Yee, K.S., Grochola, L., Hamilton, G., Grawenda, A., Bond, E.E., Taubert, H., Wurl, P., Bond, G.L., and O'Neill, E. (2012). A RASSF1A polymorphism restricts p53/p73 activation and associates with poor survival and accelerated age of onset of soft tissue sarcoma. *Cancer Res* 72, 2206-2217.

Zhao, B., Ye, X., Yu, J., Li, L., Li, W., Li, S., Lin, J.D., Wang, C.Y., Chinnaiyan, A.M., Lai, Z.C., *et al.* (2008). TEAD mediates YAP-dependent gene induction and growth control. *Genes Dev* 22, 1962-1971.

Figure legends

Figure 1. RASSF1A gets degraded in response to TGFβ. (A) Pie chart representing the functional separation of GSEA gene signatures identified in lung and breast tumour cohorts that were split on positive and negative RASSF1A mRNA or high and low promoter methylation (Tables S1 and S2). (B) Table representing overlapping signatures within each tumour type that were significantly altered in all four analyses. (NES): Nominal Enrichment Score, (FDR): False Discovery Rate, p: binomial probability. (C) Change of RASSF1A levels in HOP92 cells after treatment with TGFβ1 for the indicated times. (D) Assessment of RASSF1A levels in U2OS *TET ON* doxycycline inducible cells (*U2OS^{TetON-RASSF1A}*) treated with 1ug/ml doxycycline and TGFβ1 for the indicated times. (E) Assessment of RASSF1A levels in a TGFβ1 time course in the presence or not of MG132 or E-616451. (F) RASSF1A expression after induction with 1ug/ml doxycycline and treatment with TGFβ1 in the presence or absence of MG132. (G) U2OS cells expressing FLAG-RASSF1A were transfected with MYC-Ub, treated with TGFβ1 and FLAG-RASSF1A was immunoprecipitated (IP) to assess MYC-Ub

incorporation. (H) Western blot analysis of RASSF1A levels in NBE-1 and MCF10A cell lines after treatment with TGF β 1.

Figure 2. RASSF1A interacts with TGF β RI and is targeted by the ITCH E3 ligase for degradation. (A) RASSF1A localization in control HOP92 cells (Con) and treated with TGF β 1 for 2 h. Scale bars at 10 μ m. (B) Co-IP of FLAG-RASSF1A with endogenous TGF β RI or TGF β RII in the presence or absence of TGF β 1 (2h) in U2OS cells. (C) Graphical representation of RASSF1A mutants used for mapping RASSF1A / TGF β RI interaction and western blot analysis of MYC immunoprecipitation from the indicated inputs from U2OS cells. (D) Co-IP of ITCH and FLAG-RASSF1A in U2OS cells. (E) Assessment of RASSF1A levels in HOP92 cells treated with siITCH or siNT after treatment with TGF β 1 for the indicated times. (F) *In vivo* ubiquitination assay in U2OS cells transfected with FLAG-RASSF1A to assess MYC-Ub incorporation after treatment with siITCH or control siRNA in response to TGF β 1. (G) RASSF1A protein levels in HOP92 cells transfected with siITCH and subsequent re-expression of wild type ITCH (ITCH-WT) or a catalytically inactive mutant (ITCH-CA) in controls and cells treated with TGF β 1 for 2 h. Quantification was done relative to control. Data derived from n=3 experiments and representative blot is shown. P values derived from 2-tailed unpaired t-test of <0.05(*), <0.01(**) and <0.001(***) were considered significant. See also Figure S1

Figure 3: RASSF1A restricts TGF β signalling inhibiting YAP1 binding and nuclear accumulation of SMAD2. (A) Co-IP of YAP1 with SMAD2 or p73 in to response increasing concentrations of doxycycline and TGF β 1 treatment for 2 hours. (B) Nuclear SMAD2 in U2OS^{TetON-RASSF1A} upon treatment with doxycycline (1 μ g/ml) and stimulation with TGF β 1 for 2 h. Scale bars at 10 μ m. (C) Quantification of mean SMAD2 nuclear intensity of cells in B. Data presented as mean intensity \pm S.D from n=3 experiments. (D) Expression of *Smad7*, *PAI-1* and *CTGF* determined by qPCR from U2OS^{TetON-RASSF1A} cells treated or not with doxycycline (1 μ g/ml) and TGF β 1 for 2h. Values and error bars represent the mean \pm S.D of triplicates and are representative of 3 independent experiments. (E) Co-IP between YAP1 and SMAD2 in HOP92 cells treated with control or two different siRNA for RASSF1A and stimulated or not with TGF β 1 for 2h. (F)

Nuclear SMAD2 in *Rassf1A*^{+/+} and *Rassf1A*^{-/-} MEFs after treatment with TGFβ1 for 2 h. Scale bars at 10 μm. (G) (%) number of cells with nuclear SMAD2 in the absence of TGFβ1 stimulus. (H) Nuclear SMAD2 quantification from F. Data presented as mean intensity ± S.D from n=3 experiments. (I) Expression of *Smad7*, *PAI-1* and *CTGF* determined by qPCR from HOP92 cells treated with siRASSF1A and induced with TGFβ1 for 2h. Data show the mean ± S.D of triplicates and are representative of n=3 biological replicates. P values derived from 2-tailed unpaired t-test of <0.05(*), <0.01(**) and <0.001(***) were considered significant. See also Figure S2 and S3.

Figure 4: RASSF1A inhibits TGFβ induced invasion. (A) Boyden chamber transwell invasion assay of U2OS^{TetON-RASSF1A} cells, treated or not with TGFβ1 for 24 hours. Bar-graph shows number of invaded cells counted from four random fields. (B) Relative spheroid invasion in 3D collagen matrix of U2OS^{TetON-RASSF1A} in response to TGFβ1 stimulation for 7h. Representative images and quantification of invaded multi-cellular projections (collective) per spheroid was calculated as relative value compared to control cells are shown. Data show the mean ± S.D of n=3 experiments. (C) Boyden chamber transwell invasion assay from siRASSF1A or control treated HOP92 cells after stimulated for 24 hour with TGFβ1. Number of invaded cells and representative images are shown. Doxycycline was used at 1μg/ml for RASSF1A induction. All data represent the mean ± S.D and derive from n=3 independent experiments. P values derived from 2-tailed unpaired t-test of <0.05(*), <0.01(**) and <0.001(***) were considered significant. Scale bars at 200 μm. See also Figure S4.

Acknowledgments:

The authors would like to thank Pamela Rabbits and Andy Ryan for providing cell lines, Annie Angers, Jeff Wrana and Alex Bullock for providing constructs, Maria Laura Tognoli for useful comments on the manuscript. This work was funded by Cancer Research UK A19277.

Author contributions:

EON conceived the project and designed research. DEP designed research, performed experiments and analyzed data. DP performed the transwell invasion and spheroid

formation assays. AMG performed the GSE analysis and assisted in experiments. AGA, NV and SC assisted in experiments. EON and DEP wrote the manuscript.

Figure 1
A GSEA signatures > RASSF1 levels

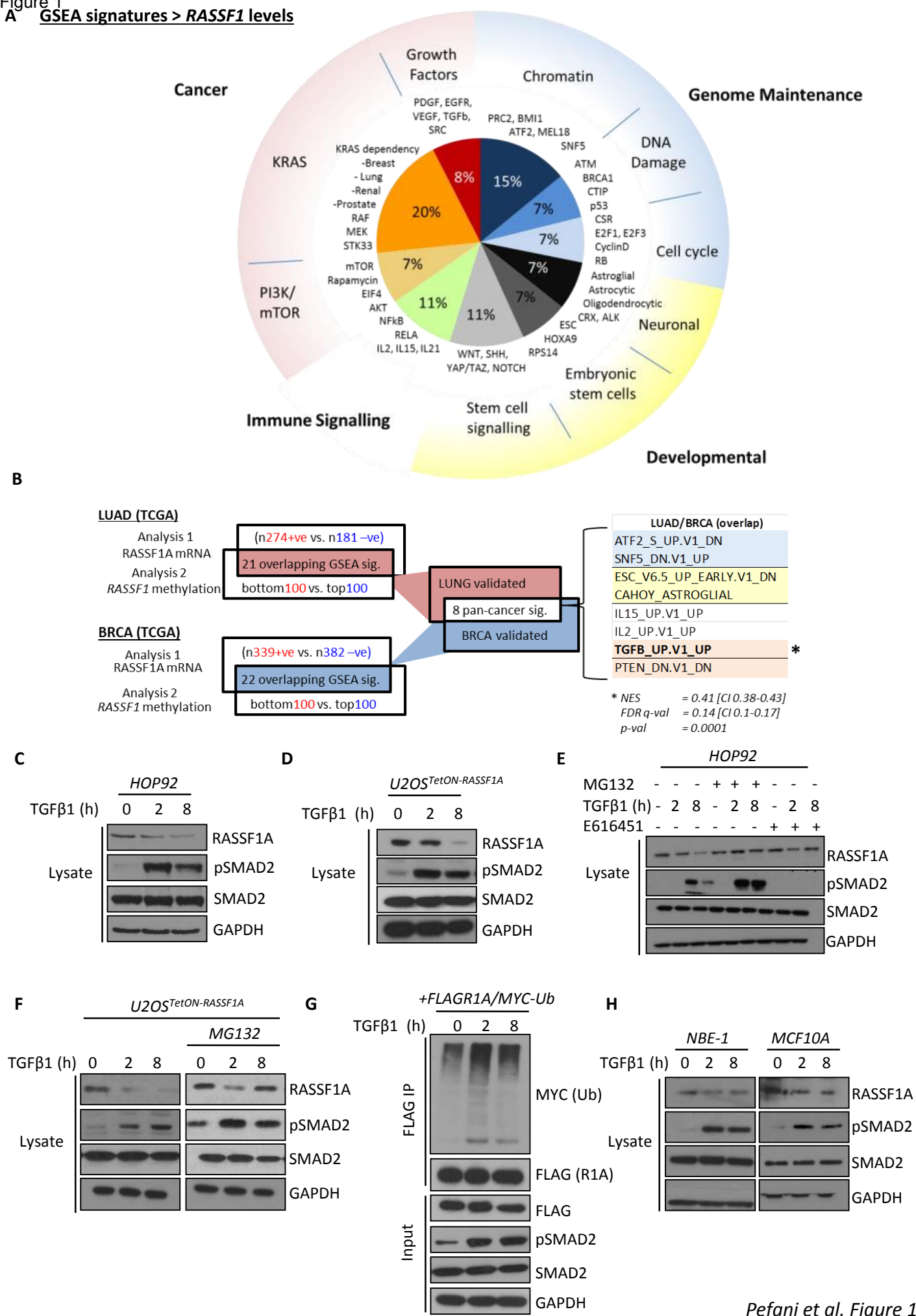


Figure 2

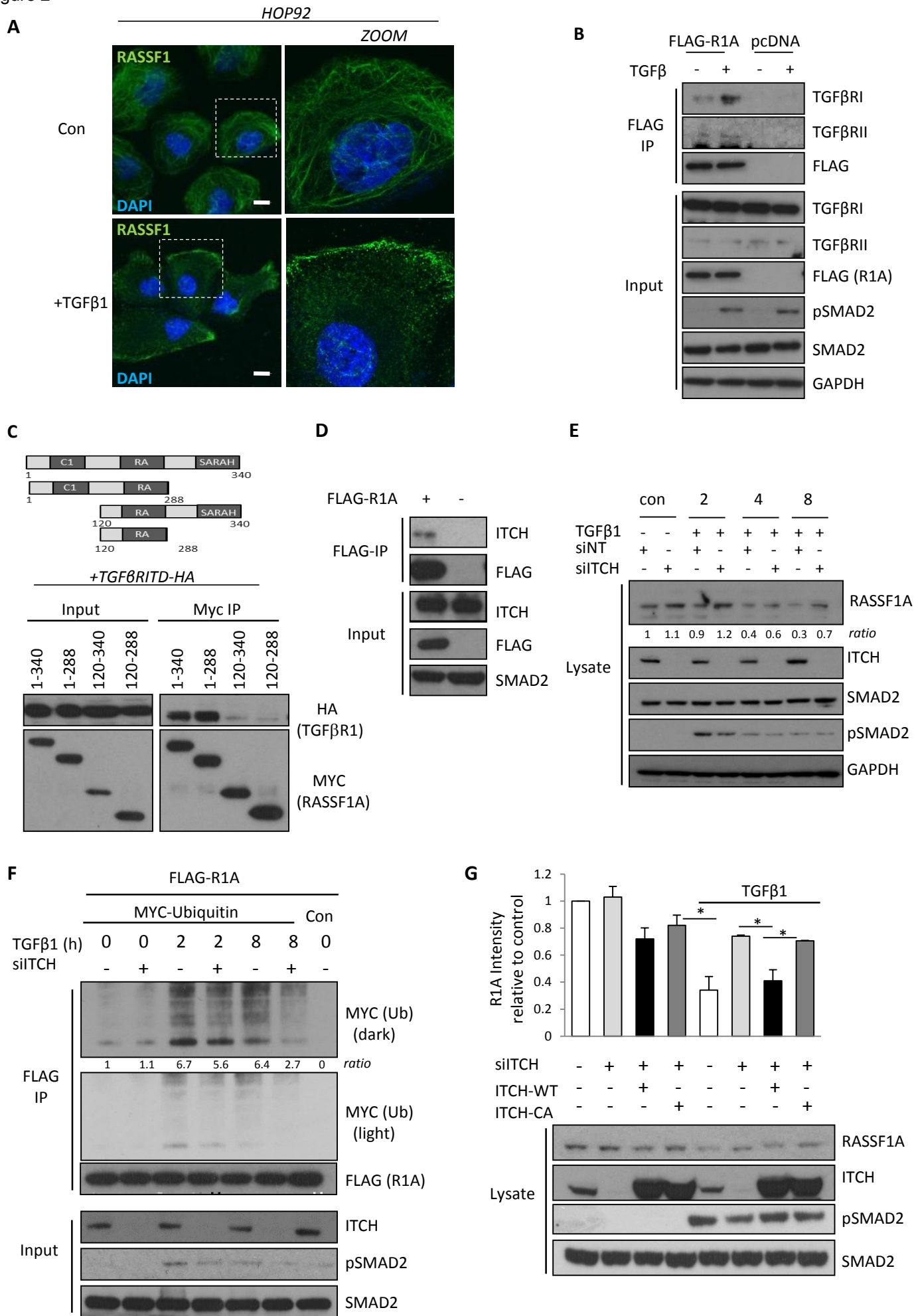


Figure 3

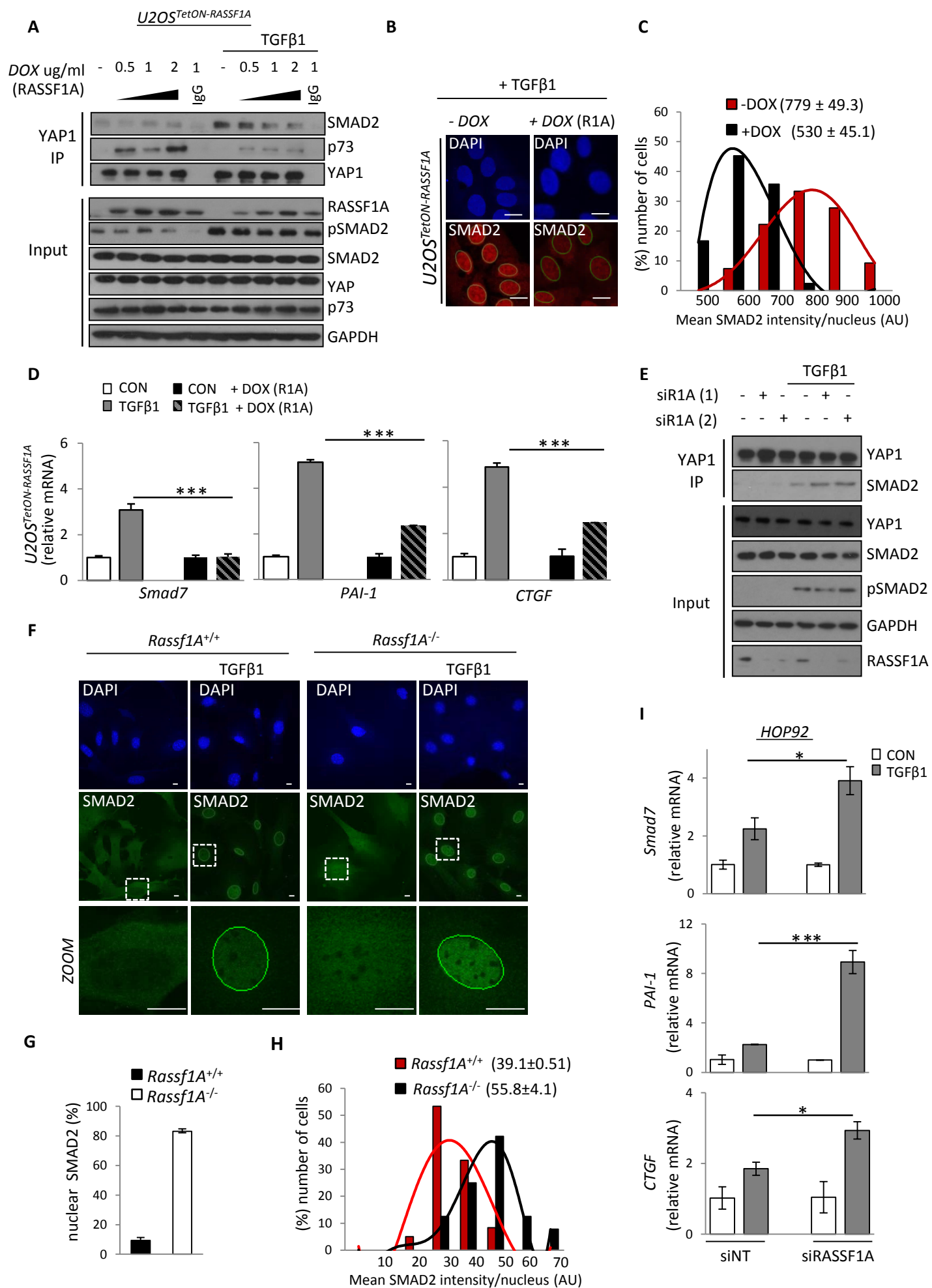
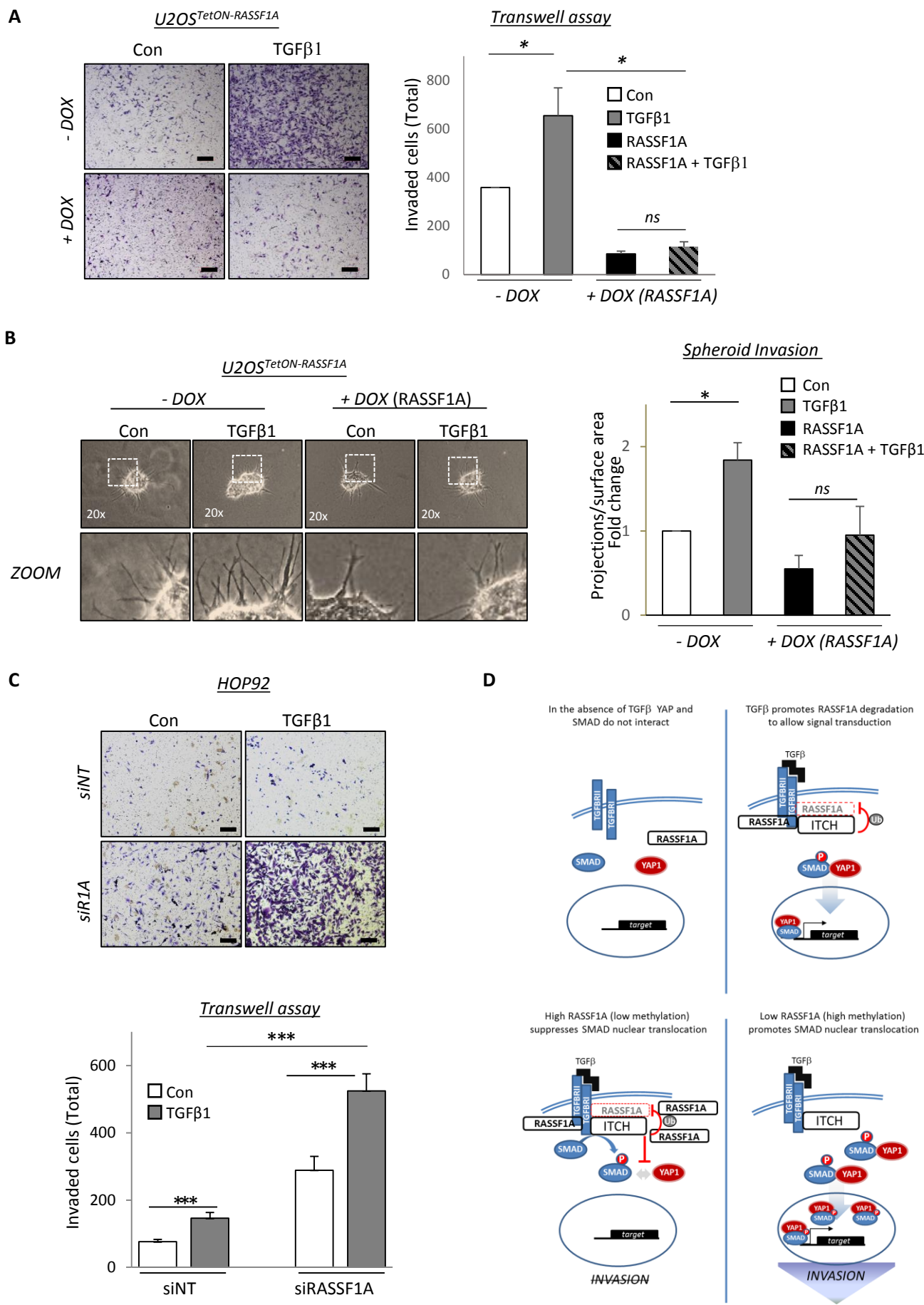
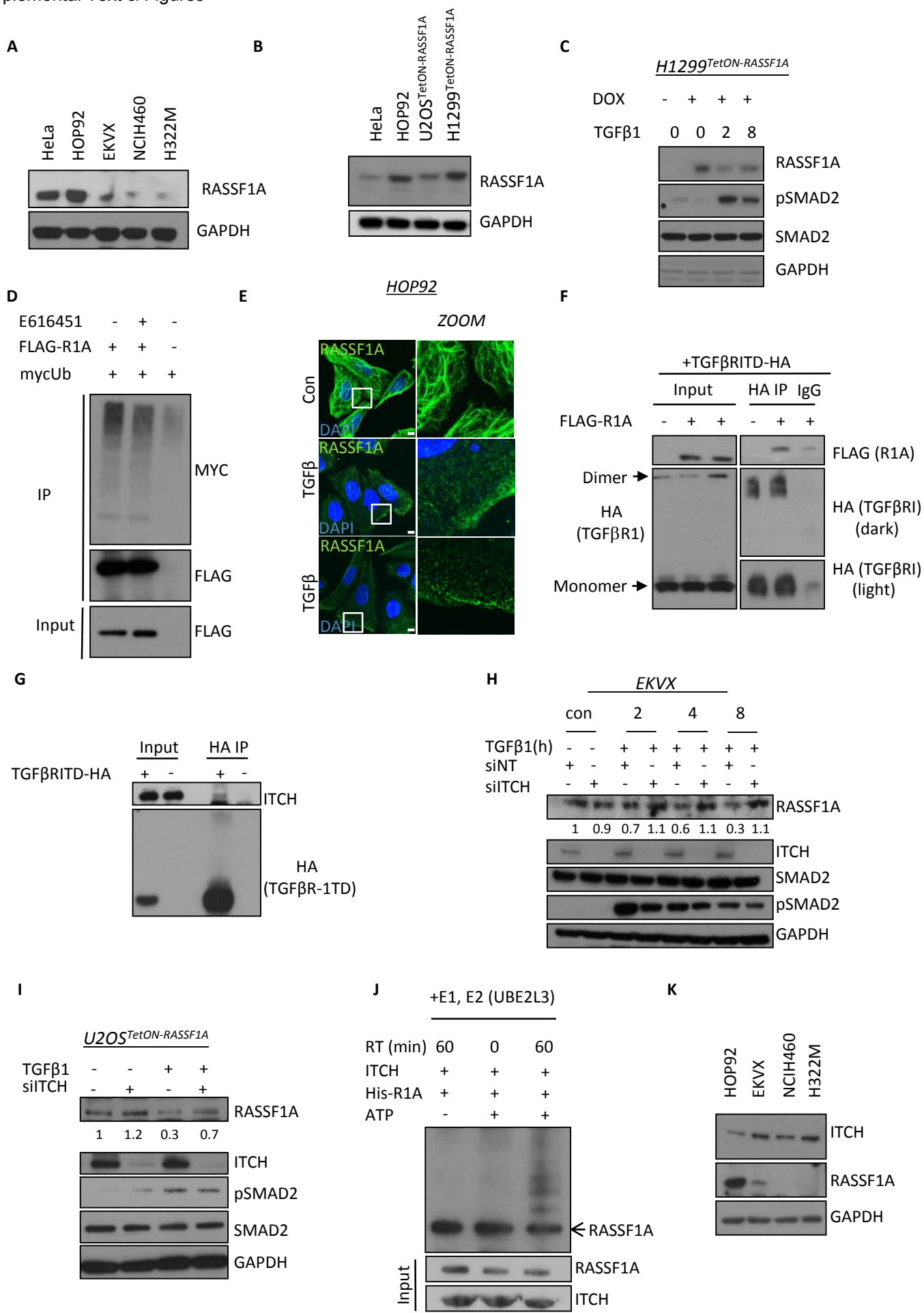
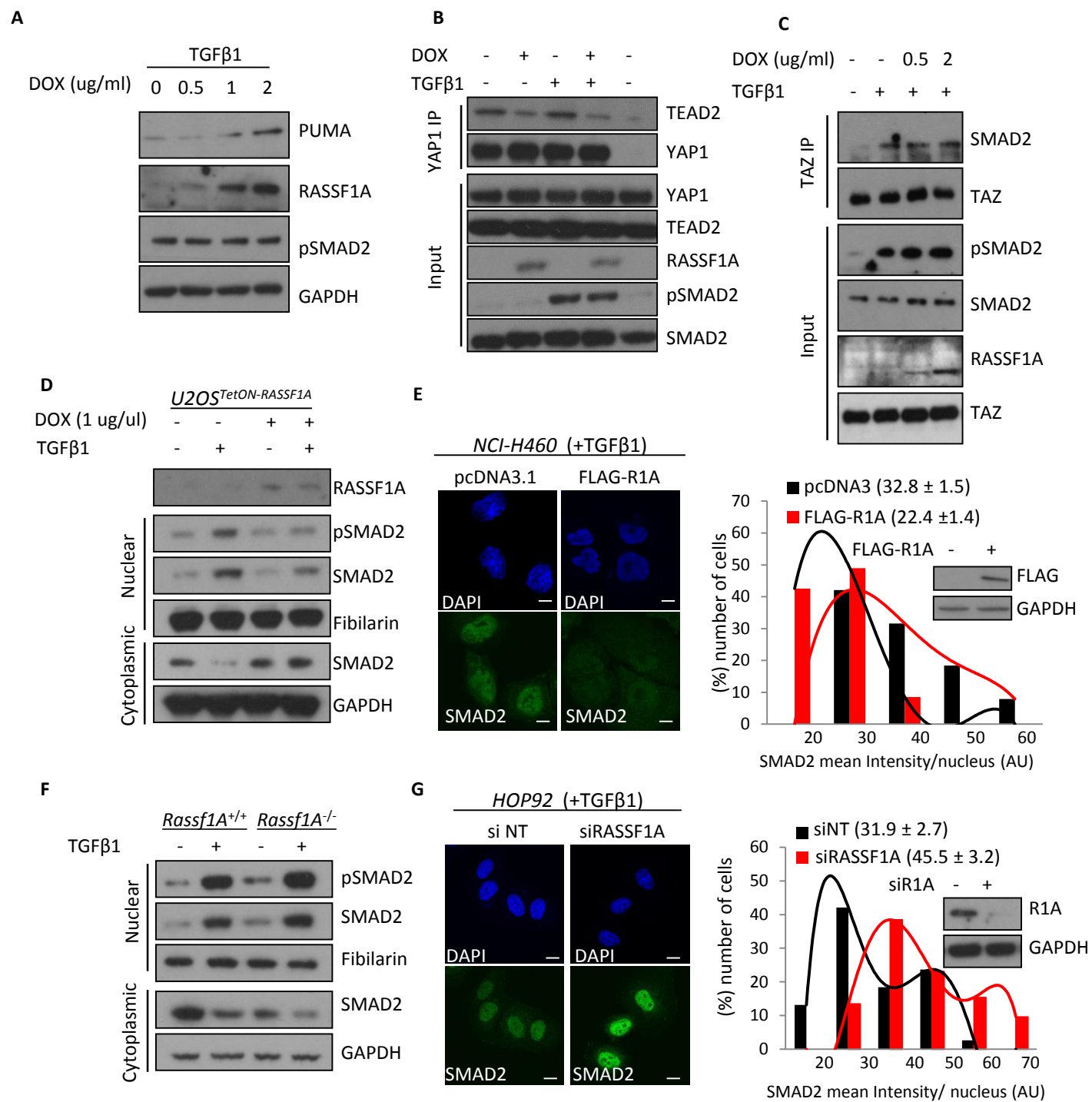
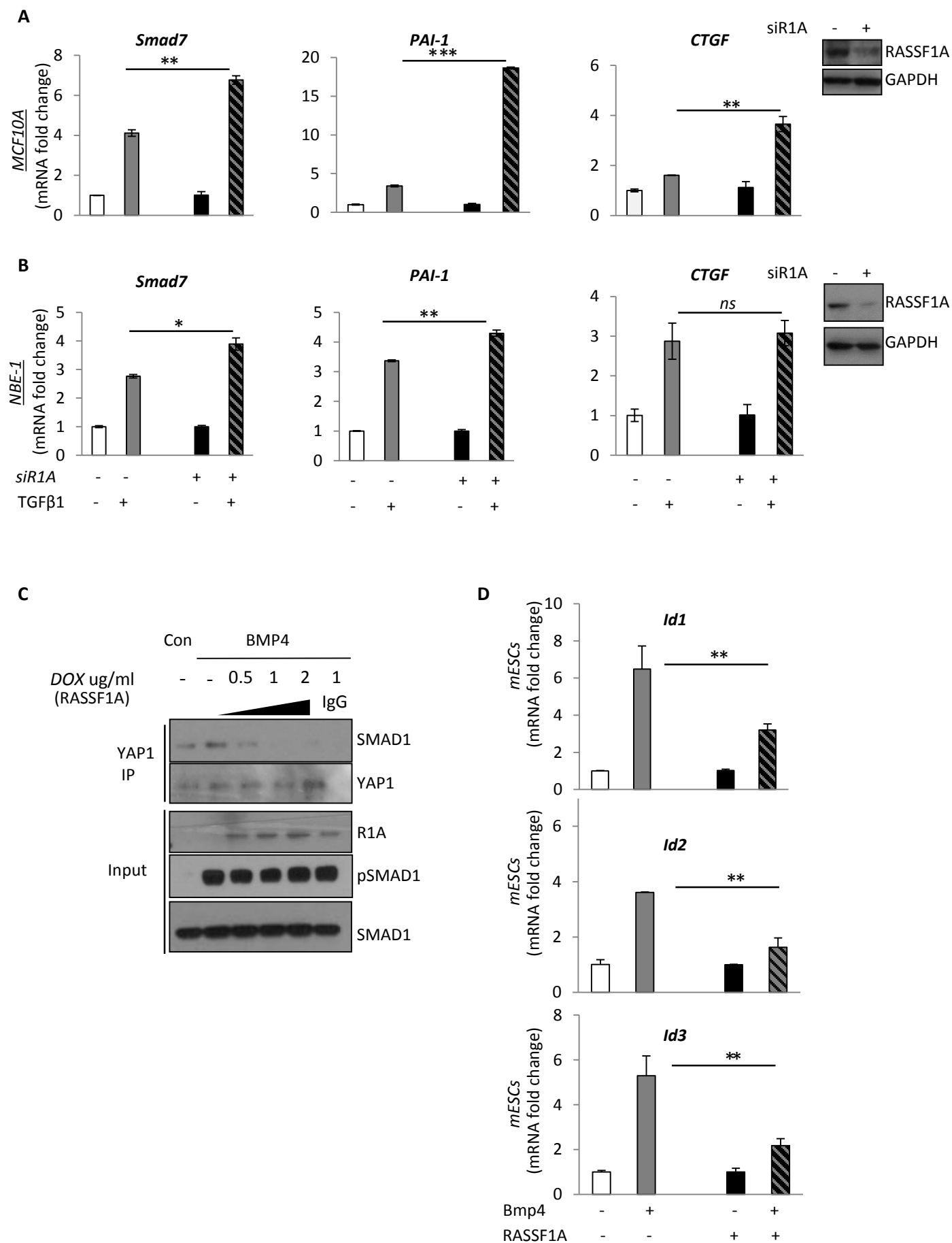


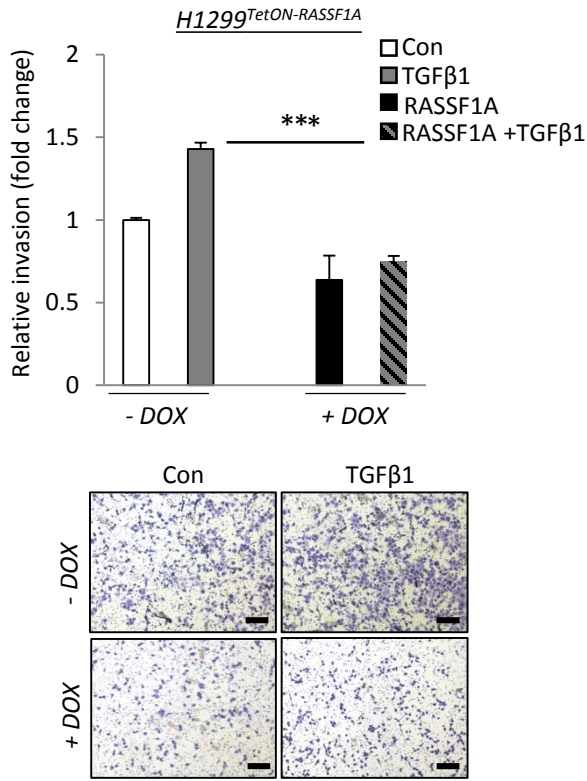
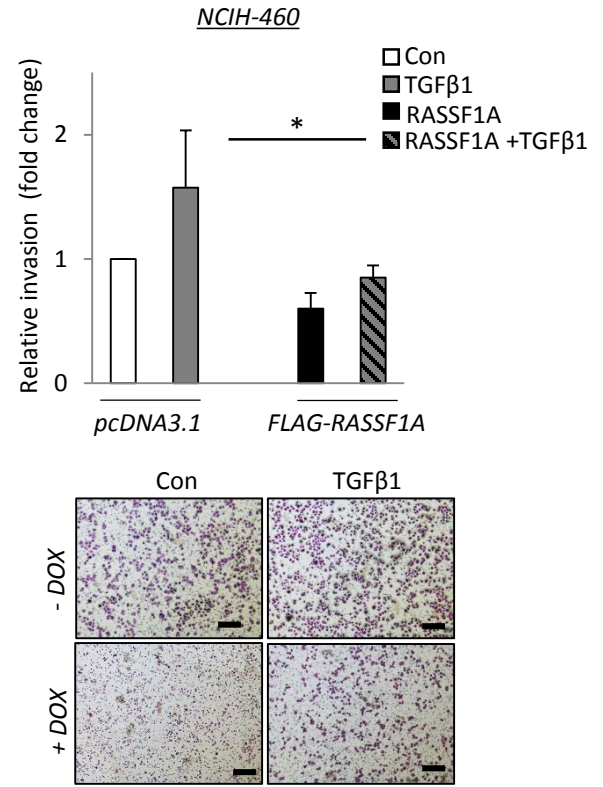
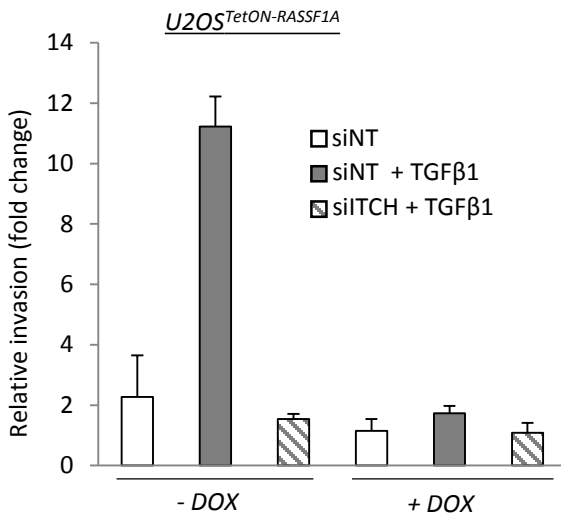
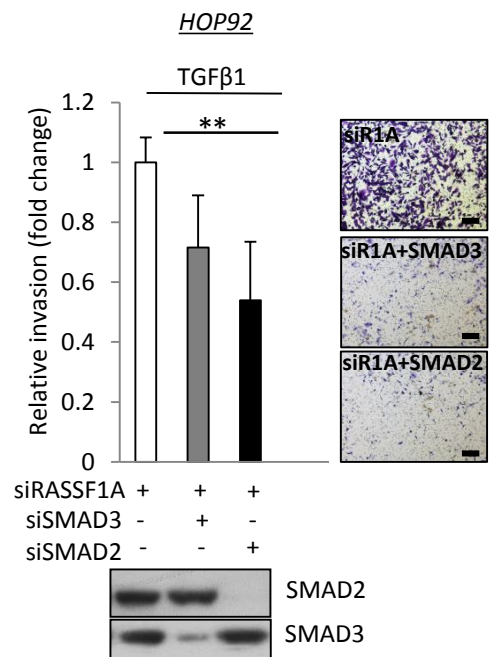
Figure 4









A**B****C****D**

LUAD – LUnG ADenocarcinoma from The Cancer Genome Analysis (TCGA)
Gene Set Enrichment Analysis (GSEA)

Analysis 1

RASSF1A mRNA expression
n= 274 +ve vs. 181 -ve

NAME	SIZE	ES	NES	NOM p-val	FDR q-val
RPS14_DN.V1_UP	189	0.68	0.68	0.00	0.05
SINGH_KRAS_DEPENDENCY_SIGNATURE_	20	0.64	0.64	0.04	0.04
HINATA_NFKB_IMMU_INF	17	0.59	0.59	0.11	0.06
HOXA9_DN.V1_UP	192	0.54	0.54	0.00	0.09
CAHOY_ASTROGLIAL	100	0.51	0.51	0.00	0.10
STK33_NOMO_UP	280	0.47	0.47	0.01	0.17
E2F1_UP.V1_DN	192	0.47	0.47	0.00	0.15
STK33_SKM_UP	269	0.46	0.46	0.00	0.15
STK33_UP	276	0.45	0.45	0.01	0.17
PTEN_DN.V2_UP	134	0.45	0.45	0.00	0.15
ESC_V6.5_UP_EARLY.V1_DN	170	0.44	0.44	0.01	0.14
BMI1_DN_MEL18_DN.V1_UP	143	0.43	0.43	0.06	0.16
EIF4E_DN	97	0.43	0.43	0.06	0.15
P53_DN.V2_UP	146	0.43	0.43	0.00	0.16
VEGF_A_UP.V1_UP	193	0.42	0.42	0.00	0.18
ATF2_S_UP.V1_DN	183	0.42	0.42	0.00	0.17
BCAT_BILD_ET_AL_UP	45	0.41	0.41	0.07	0.16
MEL18_DN.V1_UP	140	0.41	0.41	0.07	0.15
KRAS.KIDNEY_UP.V1_DN	134	0.41	0.41	0.00	0.16
KRAS.LUNG_UP.V1_DN	138	0.41	0.41	0.00	0.16
BMI1_DN.V1_UP	144	0.40	0.40	0.06	0.16
IL2_UP.V1_UP	186	0.40	0.40	0.00	0.15
KRAS.50_UP.V1_DN	46	0.40	0.40	0.09	0.15
CORDENONSI_YAP_CONSERVED_SIGNATURE	57	0.40	0.40	0.15	0.15
PRC2_SUZ12_UP.V1_DN	182	0.39	0.39	0.00	0.17
ATF2_UP.V1_DN	182	0.39	0.39	0.01	0.17
IL2_UP.V1_DN	191	0.38	0.38	0.01	0.18
SNF5_DN.V1_UP	174	0.38	0.38	0.05	0.17
TGFB_UP.V1_UP	184	0.38	0.38	0.04	0.17
KRAS.300_UP.V1_DN	136	0.38	0.38	0.02	0.17
P53_DN.V1_UP	192	0.38	0.38	0.03	0.17
MYC_UP.V1_DN	161	0.38	0.38	0.01	0.17
ESC_J1_UP_LATE.V1_UP	190	0.38	0.38	0.04	0.16
LEF1_UP.V1_UP	193	0.38	0.38	0.04	0.16
RELA_DN.V1_DN	139	0.38	0.38	0.01	0.16
MTOR_UP.N4.V1_DN	181	0.37	0.37	0.05	0.16
P53_DN.V1_DN	191	0.37	0.37	0.01	0.16
KRAS.PROSTATE_UP.V1_UP	133	0.37	0.37	0.00	0.16
RAF_UP.V1_UP	191	0.37	0.37	0.01	0.15
KRAS.AMP.LUNG_UP.V1_DN	137	0.37	0.37	0.01	0.15
GCNP_SHH_UP_LATE.V1_DN	175	0.37	0.37	0.00	0.15
CSR_LATE_UP.V1_DN	161	0.37	0.37	0.01	0.16
LEF1_UP.V1_DN	186	0.37	0.37	0.05	0.15
ATM_DN.V1_DN	144	0.37	0.37	0.01	0.15
CRX_DN.V1_DN	133	0.36	0.36	0.00	0.16
PDGF_UP.V1_DN	131	0.36	0.36	0.00	0.15
KRAS.600_UP.V1_DN	276	0.36	0.36	0.00	0.16
IL15_UP.V1_UP	183	0.36	0.36	0.01	0.17
PTEN_DN.V1_DN	178	0.36	0.36	0.02	0.17
CTIP_DN.V1_DN	133	0.35	0.35	0.01	0.17

Analysis 2

RASSF1 promoter methylation
bottom100 vs.top100

NAME	SIZE	ES	NES	NOM p-val	FDR q-val
RPS14_DN.V1_UP	189	0.68	0.68	0.00	0.05
SINGH_KRAS_DEPENDENCY_SIGNATURE_	20	0.64	0.64	0.04	0.04
HINATA_NFKB_IMMU_INF	17	0.59	0.59	0.11	0.06
HOXA9_DN.V1_UP	192	0.54	0.54	0.00	0.09
CAHOY_ASTROGLIAL	100	0.51	0.51	0.00	0.10
STK33_NOMO_UP	280	0.47	0.47	0.01	0.17
E2F1_UP.V1_DN	192	0.47	0.47	0.00	0.15
STK33_SKM_UP	269	0.46	0.46	0.00	0.15
STK33_UP	276	0.45	0.45	0.01	0.17
PTEN_DN.V2_UP	134	0.45	0.45	0.00	0.15
ESC_V6.5_UP_EARLY.V1_DN	170	0.44	0.44	0.01	0.14
BMI1_DN_MEL18_DN.V1_UP	143	0.43	0.43	0.06	0.16
EIF4E_DN	97	0.43	0.43	0.06	0.15
P53_DN.V2_UP	146	0.43	0.43	0.00	0.16
VEGF_A_UP.V1_UP	193	0.42	0.42	0.00	0.18
ATF2_S_UP.V1_DN	183	0.42	0.42	0.00	0.17
BCAT_BILD_ET_AL_UP	45	0.41	0.41	0.07	0.16
MEL18_DN.V1_UP	140	0.41	0.41	0.07	0.15
KRAS.KIDNEY_UP.V1_DN	134	0.41	0.41	0.00	0.16
KRAS.LUNG_UP.V1_DN	138	0.41	0.41	0.00	0.16
BMI1_DN.V1_UP	144	0.40	0.40	0.06	0.16
IL2_UP.V1_UP	186	0.40	0.40	0.00	0.15
KRAS.50_UP.V1_DN	46	0.40	0.40	0.09	0.15
CORDENONSI_YAP_CONSERVED_SIGNATURE	57	0.40	0.40	0.15	0.15
PRC2_SUZ12_UP.V1_DN	182	0.39	0.39	0.00	0.17
ATF2_UP.V1_DN	182	0.39	0.39	0.01	0.17
IL2_UP.V1_DN	191	0.38	0.38	0.01	0.18
SNF5_DN.V1_UP	174	0.38	0.38	0.05	0.17
TGFB_UP.V1_UP	184	0.38	0.38	0.04	0.17
KRAS.300_UP.V1_DN	136	0.38	0.38	0.02	0.17
P53_DN.V1_UP	192	0.38	0.38	0.03	0.17
MYC_UP.V1_DN	161	0.38	0.38	0.01	0.17
ESC_J1_UP_LATE.V1_UP	190	0.38	0.38	0.04	0.16
LEF1_UP.V1_UP	193	0.38	0.38	0.04	0.16
RELA_DN.V1_DN	139	0.38	0.38	0.01	0.16
MTOR_UP.N4.V1_DN	181	0.37	0.37	0.05	0.16
P53_DN.V1_DN	191	0.37	0.37	0.01	0.16
KRAS.PROSTATE_UP.V1_UP	133	0.37	0.37	0.00	0.16
RAF_UP.V1_UP	191	0.37	0.37	0.01	0.15
KRAS.AMP.LUNG_UP.V1_DN	137	0.37	0.37	0.01	0.15
GCNP_SHH_UP_LATE.V1_DN	175	0.37	0.37	0.00	0.15
CSR_LATE_UP.V1_DN	161	0.37	0.37	0.01	0.16
LEF1_UP.V1_DN	186	0.37	0.37	0.05	0.15
ATM_DN.V1_DN	144	0.37	0.37	0.01	0.15
CRX_DN.V1_DN	133	0.36	0.36	0.00	0.16
PDGF_UP.V1_DN	131	0.36	0.36	0.00	0.15
KRAS.600_UP.V1_DN	276	0.36	0.36	0.00	0.16
IL15_UP.V1_UP	183	0.36	0.36	0.01	0.17
PTEN_DN.V1_DN	178	0.36	0.36	0.02	0.17
CTIP_DN.V1_DN	133	0.35	0.35	0.01	0.17

c6.all.v5.0.symbols.gmt [oncogenic signatures]

BRCA – BReast Cancer from The Cancer Genome Analysis (TCGA)
Gene Set Enrichment Analysis (GSEA)

Analysis 1

RASSF1A mRNA expression
n= 339 +ve vs. 382 -ve

Analysis 2

RASSF1 promoter methylation
bottom100 vs.top100

NAME	SIZE	ES	NES	NOM p-val	FDR q-val	NAME	SIZE	ES	NES	NOM p-val	FDR q-val
HINATA_NFKB_IMMUN_INF	17	0.68	0.68	0.07	0.05	HINATA_NFKB_IMMUN_INF	17	0.74	0.74	0.04	0.03
RPS14_DN.V1_UP	189	0.53	0.53	0.01	0.16	RPS14_DN.V1_UP	189	0.59	0.59	0.00	0.10
CORDENONSI_YAP_CONSERVED_SIGNATURE	57	0.52	0.52	0.02	0.15	CORDENONSI_YAP_CONSERVED_SIGNATURE	57	0.57	0.57	0.01	0.08
ESC_V6.5_UP_EARLY.V1_DN	170	0.51	0.51	0.00	0.12	RAF_UP.V1_UP	191	0.55	0.55	0.00	0.08
MEL18_DN.V1_UP	140	0.51	0.51	0.00	0.11	BMI1_DN_MEL18_DN.V1_UP	143	0.54	0.54	0.00	0.07
VEGF_A_UP.V1_UP	193	0.49	0.49	0.00	0.11	SNF5_DN.V1_UP	174	0.51	0.51	0.00	0.08
CYCLIN_D1_UP.V1_UP	185	0.49	0.49	0.00	0.10	MEL18_DN.V1_UP	140	0.51	0.51	0.00	0.07
SNF5_DN.V1_UP	174	0.48	0.48	0.00	0.10	EGFR_UP.V1_UP	190	0.51	0.51	0.00	0.07
BMI1_DN_MEL18_DN.V1_UP	143	0.48	0.48	0.01	0.09	BMI1_DN.V1_UP	144	0.51	0.51	0.00	0.06
PRC2_EDD_UP.V1_UP	191	0.48	0.48	0.00	0.08	CSR_EARLY_UP.V1_UP	159	0.50	0.50	0.00	0.06
BMI1_DN.V1_UP	144	0.48	0.48	0.02	0.08	SINGH_KRAS_DEPENDENCY_SIGNATURE_	20	0.50	0.50	0.10	0.06
CAHOY_ASTROGLIAL	100	0.48	0.48	0.00	0.07	CAHOY_ASTROGLIAL	100	0.48	0.48	0.00	0.07
LEF1_UP.V1_UP	193	0.47	0.47	0.00	0.08	IL2_UP.V1_UP	186	0.48	0.48	0.00	0.06
IL2_UP.V1_UP	186	0.46	0.46	0.00	0.09	LEF1_UP.V1_UP	193	0.46	0.46	0.00	0.08
IL15_UP.V1_UP	183	0.45	0.45	0.00	0.09	IL15_UP.V1_UP	183	0.46	0.46	0.00	0.08
PIGF_UP.V1_DN	186	0.44	0.44	0.00	0.11	PTEN_DN.V2_UP	134	0.45	0.45	0.00	0.08
AKT_UP.V1_DN	186	0.44	0.44	0.00	0.10	ALK_DN.V1_UP	136	0.44	0.44	0.00	0.09
JNK_DN.V1_DN	183	0.44	0.44	0.00	0.10	ESC_V6.5_UP_EARLY.V1_DN	170	0.44	0.44	0.03	0.10
P53_DN.V2_UP	146	0.43	0.43	0.00	0.10	KRAS.LUNG_UP.V1_UP	137	0.42	0.42	0.00	0.13
TGFB_UP.V1_UP	184	0.43	0.43	0.04	0.10	TGFB_UP.V1_UP	184	0.41	0.41	0.04	0.14
KRAS.S0_UP.V1_DN	46	0.43	0.43	0.02	0.10	SIRNA_EIF4GI_DN	94	0.41	0.41	0.03	0.14
KRAS.AMP.LUNG_UP.V1_DN	137	0.42	0.42	0.00	0.11	GLI1_UP.V1_UP	27	0.41	0.41	0.04	0.13
GCNP_SHH_UP_LATE.V1_DN	175	0.42	0.42	0.00	0.10	P53_DN.V2_UP	146	0.41	0.41	0.00	0.13
ATF2_S_UP.V1_DN	183	0.42	0.42	0.00	0.10	HOUA9_DN.V1_UP	192	0.40	0.40	0.04	0.15
CSR_LATE_UP.V1_DN	161	0.41	0.41	0.01	0.11	RB_P107_DN.V1_UP	136	0.40	0.40	0.17	0.14
SRC_UP.V1_UP	163	0.41	0.41	0.01	0.11	CAHOY_OLIGODENDROCYTIC	97	0.40	0.40	0.01	0.14
BCAT_BILD_ET_AL_UP	45	0.41	0.41	0.04	0.11	MEK_UP.V1_UP	194	0.40	0.40	0.01	0.13
ALK_DN.V1_UP	136	0.41	0.41	0.01	0.11	RELA_DN.V1_UP	149	0.40	0.40	0.00	0.13
PTEN_DN.V2_UP	134	0.41	0.41	0.01	0.11	P53_DN.V1_DN	191	0.40	0.40	0.00	0.13
RAPA_EARLY_UP.V1_DN	187	0.41	0.41	0.00	0.11	CRX_DN.V1_DN	133	0.40	0.40	0.01	0.13
KRAS.300_UP.V1_DN	136	0.40	0.40	0.00	0.11	KRAS.LUNG.BREAST_UP.V1_UP	138	0.39	0.39	0.01	0.13
MTOR_UP.V1_DN	179	0.40	0.40	0.00	0.12	CAHOY_ASTROCYTIC	100	0.39	0.39	0.03	0.13
RB_P130_DN.V1_UP	128	0.40	0.40	0.03	0.12	CYCLIN_D1_UP.V1_UP	185	0.39	0.39	0.01	0.13
ESC_I1_UP_EARLY.V1_DN	174	0.40	0.40	0.00	0.12	JNK_DN.V1_UP	183	0.39	0.39	0.01	0.13
ESC_V6.5_UP_LATE.V1_DN	177	0.39	0.39	0.01	0.12	CSR_LATE_UP.V1_UP	170	0.39	0.39	0.14	0.12
KRAS.LUNG.BREAST_UP.V1_UP	138	0.39	0.39	0.01	0.11	STK33_NOMO_UP	280	0.39	0.39	0.05	0.12
WNT_UP.V1_UP	177	0.39	0.39	0.00	0.12	PTEN_DN.V1_DN	178	0.39	0.39	0.00	0.12
KRAS.LUNG_UP.V1_UP	137	0.39	0.39	0.02	0.12	PRC2_EZH2_UP.V1_DN	192	0.39	0.39	0.02	0.12
PTEN_DN.V1_DN	178	0.39	0.39	0.00	0.11	ATM_DN.V1_DN	144	0.38	0.38	0.01	0.13
KRAS.KIDNEY_UP.V1_DN	134	0.39	0.39	0.00	0.12	ATF2_UP.V1_DN	182	0.38	0.38	0.01	0.13
MEK_UP.V1_UP	194	0.39	0.39	0.03	0.12	KRAS.S0_UP.V1_UP	48	0.38	0.38	0.07	0.13
PTEN_DN.V2_DN	137	0.38	0.38	0.00	0.12	JNK_DN.V1_DN	183	0.38	0.38	0.00	0.13
NOTCH_DN.V1_DN	181	0.38	0.38	0.00	0.12	MYC_UP.V1_DN	161	0.38	0.38	0.01	0.13
RB_P107_DN.V1_UP	136	0.38	0.38	0.21	0.12	ESC_V6.5_UP_LATE.V1_DN	177	0.38	0.38	0.01	0.13
PDGF_ERK_DN.V1_DN	145	0.38	0.38	0.01	0.12	STK33_UP	276	0.37	0.37	0.06	0.13
CRX_NRL_DN.V1_UP	137	0.38	0.38	0.00	0.12	SRC_UP.V1_DN	165	0.37	0.37	0.00	0.14
ATF2_UP.V1_UP	185	0.38	0.38	0.00	0.11	KRAS.BREAST_UP.V1_UP	135	0.37	0.37	0.01	0.14
WNT_UP.V1_DN	169	0.38	0.38	0.00	0.12	P53_DN.V1_UP	192	0.37	0.37	0.03	0.14
IL21_UP.V1_UP	182	0.38	0.38	0.01	0.12	ATF2_S_UP.V1_DN	183	0.37	0.37	0.02	0.14
CYCLIN_D1_KE_V1_UP	187	0.37	0.37	0.00	0.12						

c6.all.v5.0.symbols.gmt [oncogenic signatures]

Supplemental information

Supplemental Figure Legends

Figure S1 (related to Figure 1 and 2): RASSF1A interacts with TGF β RI and gets degraded by ITCH in response to TGF β signalling. (A) RASSF1A expression levels in the NCI-60 lung cancer cell lines. (B) RASSF1A levels in the indicated cell lines. U2OS^{TetON-RASSF1A} and H1299^{TetON-RASSF1A} were induced with 0.5 μ g/ml of doxycycline. (C) Western Blot analysis of RASSF1A levels in response to TGF β 1 in H1299 cells that express RASSF1A under the tetracyclin promoter in the presence of 1 μ g/ml of doxycycline. (D) *In vivo* Ubiquitination assay in FLAG-RASSF1A transiently transfected U2OS cells treated or not with TGF β RI kinase inhibitor II (E616451). (E) RASSF1A localisation in control and TGF β 1 treated cells. Scale bars at 10 μ m. (F) Co-immunoprecipitation (Co-IP) between FLAG-RASSF1A and the constantly active TGF β Receptor I (TGF β RI^{TD}-HA) in U2OS cells. (G) Interaction between endogenous ITCH and TGF β RI^{TD}-HA in U2OS cells. (H) RASSF1A protein levels in EKVX lung cancer cells treated with siRNA against ITCH or control siRNA after addition of TGF β 1 for the indicated times. (I) U2OS^{TetON-RASSF1A} cells were induced with 1 μ g/ml doxycycline, treated with siRNA against ITCH or Non-Targeting siRNA and stimulated with TGF β 1 for 2 h. Total cell extracts were analysed with western blotting for the indicated antibodies. (J) *In vitro* ubiquitination assay with purified RASSF1 and ITCH proteins. RT: Reaction Time. (K) ITCH protein levels in the NCI-60 lung cancer cell lines.

Figure S2 (related to Figure 3): RASSF1A controls SMAD2 nuclear accumulation. (A) PUMA protein levels in U2OS^{TetON-RASSF1A} cells treated with increasing concentrations of doxycycline and stimulated with TGF β 1 for 2 h. (B) Co-IP between YAP and TEAD2 in the U2OS^{TetON-RASSF1A} cells in the presence or not of 1 μ g/ml doxycycline after treatment or not with TGF β 1 for 2h. (C) Co-IP between TAZ and SMAD2 in U2OS^{TetON-RASSF1A} cells that were treated with the indicated concentrations of doxycycline and induced or not with TGF β 1 for 2h. (D) U2OS^{TetON-RASSF1A} cells were treated or not with TGF β 1 for 2 h prior to nuclear/cytoplasmic separation. Total cell lysates, nuclear and cytoplasmic fractions were analysed by western blotting with the indicated antibodies. (E) Quantification of mean SMAD2 nuclear intensity and representative images from NCI-H460 cells transiently transfected with FLAG-RASSF1A or control plasmid and treated or not with TGF β 1 for 2h. Data presented as mean intensity

and \pm S.D from n=3 experiments. Scale bars at 10 μ m. (F) *Rassf1A*^{+/+} and *Rassf1A*^{-/-} MEFS were treated with TGF β 1 for 2h followed by a nuclear-cytoplasmic fractionation. Nuclear and cytoplasmic fractions were blotted for the indicated antibodies. (G) Quantification of mean SMAD2 nuclear intensity and representative images from HOP92 cells treated with siRASSF1A or control siRNA and stimulated or not with TGF β 1 for 2h. Data presented as mean intensity and \pm S.D from n=3 experiments. Scale bars at 10 μ m. P values derived from 2-tailed unpaired t-test of <0.05(*), <0.01(**) and <0.001(***) were considered significant.

Figure S3 (related to Figure 3): RASSF1A regulates the transcriptional output of the TGF β superfamily. (A) Expression of *Smad7*, *PAI-1* and *CTGF* determined by qPCR from MCF10A cells treated with siRASSF1A and induced with TGF β 1. Values and error bars represent the mean \pm S.D of triplicates and are representative of at least two independent experiments. (B) Expression of *Smad7*, *PAI-1* and *CTGF* determined by qPCR from NBE-1 cells treated with siRASSF1A and induced with TGF β 1. Values and error bars represent the mean \pm S.D of triplicates and are representative of at least two independent experiments. (C) Co-IP between YAP and SMAD1 in U2OS^{TetON-RASSF1A} cells after treatment with increasing concentrations of doxycycline and BMP4 induction for 2h. (D) E14 mouse embryonic stem cells were transfected with ZsGreen-RASSF1A and treated with BMP4 for 2 h. Expression of the *Id1*, *Id2* and *Id3*, Bmp4 transcriptional targets was assessed by qPCR. Values and error bars represent the mean \pm S.D of triplicates and are representative of at least two independent experiments. P values derived from 2-tailed unpaired t-test of <0.05(*), <0.01(**) and <0.001(***) were considered significant.

Figure S4 (related to Figure 4): RASSF1A controls TGF β induced invasion. (A) Boyden chamber transwell assay of H1299 cells expressing RASSF1A under the tetracyclin promoter, were treated with 1 μ g/ml of doxycycline and stimulated or not with TGF β 1 for 24 hours. Representative images are shown. (B) Transwell invasion assay of NCI-H460 cells transiently transfected with FLAG-RASSF1A or control plasmid after treatment or not with TGF β 1 for 24 hours. Representative images are shown. (C) Transwell invasion assay of U2OS^{TetON-RASSF1A} cells that were treated or not with 1 μ g/ml doxycycline and/or siITCH prior to TGF β 1 addition for 24 hours. (D) Transwell invasion assay of HOP92 cells treated for siRASSF1A and siSMAD3 or siSMAD2 and stimulated with TGF β 1 for 24 hours. Representative images are shown. Invading cells were counted from four random fields, and data represent the mean \pm S.D of

n=3 experiments. P values derived from 2-tailed unpaired t-test of <0.05(*), <0.01(**) and <0.001(***) were considered significant. Scale bars at 200 um.

Table S1 (related to Figure 1): Gene Set Enrichment Analysis scores for mRNA Analysis 1 (RASSF1A mRNA positive [>0] versus negative [$=0$]) and methylation Analysis 2 (*RASSF1* methylation top100 versus bottom100) of lung adenocarcinoma from the TCGA (LUAD). Data indicates Enrichment Score (ES); Nominal Enrichment Score (NES); p-value; False Discovery Rate (FDR <0.15).

Table S2 (related to Figure 1): Gene Set Enrichment Analysis scores for mRNA Analysis 1 (RASSF1A mRNA positive [>0] versus negative [$=0$]) and methylation Analysis 2 (*RASSF1* methylation top100 versus bottom100) of breast cancer from the TCGA (BRCA). Data indicates Enrichment Score (ES); Nominal Enrichment Score (NES); nominal p-value; False Discovery Rate (FDR <0.15).

Supplemental Experimental Procedures

Tissue Culture and treatments.

U2OS and H1299 cells expressing RASSF1A under the tetracycline promoter were previously described (van der Weyden et al., 2012; Yee et al., 2012). RASSF1A expression was induced after treatment with 1 μ g/ml with doxycycline (unless indicated otherwise) for 24 hours. *Rassf1A*^{-/-} MEFS were previously described in (Pefani et al., 2014). U2OS, HOP92, EKVX and NCI-H460 cells were cultured with 10% FBS in 5% CO₂ and 20% O₂ at 37 °C. E14 mESCs were cultured with propagation medium supplemented with LIF in 5% CO₂ and 20% O₂ at 37 °C. NBE-1 cells were kindly provided by Pamela Rabbits and cultured in advanced DMEM in the presence of 5% FBS in 5% CO₂ and 20% O₂ at 37 °C. MCF10A cells were cultured in DMEM/F12 supplemented 2% HS, 20ng/ml EGF, 0.5 mg/ml Hydrocortisone, 100 ng/ml Cholera Toxin, and 10 ng/ml Insulin. For TGF β signalling activation, cells were treated with 10 ng/ml TGF β 1 (Peprotech) for 2 hours, unless indicated otherwise. For BMP signalling activation, cells were treated with 25 ng/ml BMP4 (Peprotech) for 2 hours.

Immunoprecipitation and immunoblotting

Cells were lysed in 1% NP-40 lysis buffer (150 mM NaCl, 20 mM HEPES, 0.5 mM EDTA, phosphatase inhibitors, complete proteinase inhibitor cocktail (Roche)). Total cell extracts were incubated for 3 hours with 20 μ l protein G Dynabeads (Invitrogen) and 2 μ g of the indicated antibodies at 4 °C. Immunoprecipitates were washed 3 times in lysis buffer. Total cell extracts (corresponding to 10% of the immunoprecipitate) and immunoprecipitates were resolved in 4–12% Bis-Tris Nu-PAGE gels (Invitrogen) and transferred into PVDF membrane (Millipore) before immunoblotting with the appropriate antibodies overnight at 4 °C. Primary antibody detection was achieved with peroxide-conjugated anti-rabbit or anti-mouse antibodies (Jackson ImmunoResearch) and exposure to X-ray film (Kodak). To quantify the bands obtained with western blot analysis, we used ImageJ software. All bands were normalized against the loading controls.

In vivo Ubiquitination assay

U2OS were transfected with MYC-tagged Ubiquitin and FLAG-RASSF1A using Lipofectamine 2000 (Invitrogen). When RASSF1A ubiquitination was tested in the absence of ITCH, cells

were treated with ITCH or control siRNA 24 hours prior to plasmid transfection. 24 hours following plasmid transfection cells were treated with TGFβ1 (10 ng/ml) in the presence of 10 μM MG-132. Cells were lysed in RIPA buffer (50 mM Tris pH 8.0, 150 mM NaCl, 1 % (v/v) Triton X 100, 0.5 % (w/v) sodium deoxycholate, 0.1 % (w/v) SDS, 1 mM EDTA, 1 mM EGTA, 50 mM NaF, 1 mM Na3VO4, 10 mM sodium β-glycerophosphate, 5 mM sodium pyrophosphate and 'Complete' proteinase inhibitor cocktail EDTA Free supplemented with 1 mM N-Ethylmaleimide). Cell lysates were subjected to immunoprecipitation using a FLAG-tag antibody as described above. Cell lysates and immunoprecipitates were analysed in Western Blotting.

In vitro Ubiquitination assay

To assess RASSF1A ubiquitination by ITCH E3 ligase the ITCH/AIP4 Ubiquitin Ligase Kit was used (BostonBiochem). Purified RASSF1A (His tag) protein was purchased by Fitzgerald.

Immunofluorescence

Cells were treated as indicated and fixed with 4% paraformaldehyde, permeabilized with 0.3% Triton X-100 and blocked with 2% BSA in 1×PBS. Coverslips were incubated with the indicated antibodies in blocking solution overnight at 4°C, washed and stained with secondary anti-rabbit or anti-mouse IgG conjugated with Alexa-Fluor 488 or Alexa-Fluor 594 before washing with 0.1% Tween in PBS and stained with DAPI. Cells were analysed using an LSM780 (Carl Zeiss Microscopy) confocal microscope or Nikon 90i wide-field microscope. For each condition, 200–300 cells were scored and quantified for nuclear SMAD2 using the NIS-elements software (Nikon). For RASSF1A visualisation cells were fixed with ice cold MeOH and blocked with 0.2 % Fish Gelatine. RASSF1A (eB114-10H1, ebioscience) was used in 1:100.

Quantitative real time PCR analysis:

RNA extraction, reverse transcription and qPCR reaction was performed using the Ambion® Power SYBR® Green Cells-to-Ct™ kit following manufacturer's instructions (Thermo) in a 7500 FAST Real-Time PCR thermocycler with v2.0.5 software (Applied Biosystems). mRNA fold change was calculated using a $2^{-(\Delta\Delta Ct)}$ method in relation to the 18S or GAPDH reference genes (all primers used are listed below).

Spheroids invasion in 3D collagen matrix

U2OS multicellular tumour spheroids were generated by using the hanging-drop method (Foty, 2011). In brief, U2OS^{TetON-RASSF1A} cells were induced or not with 1 ug/ml doxycycline for 24 hours before spheroid formation. Cells were detached 2mM EDTA and re-suspended in medium supplemented with methylcellulose (20%; Sigma-Aldrich) and Matrigel (1%, BD Biosciences, Growth factor reduced) and incubated as hanging droplets (25 µl) containing 2000 cells for 48 h to ensure multicellular aggregation. Then U2OS spheroids were washed with the completed medium, collected and mixed with a solution of rat tail collagen (SERVA Electrophoresis) (2.0 mg/ml), which was pipetted as a 3D spheroids-matrix gel, polymerized at 37°C and replaced with medium containing 25 ng/ml TGFβ. Spheroids were imaged and examined for invasive features under bright-field microscope 7 hours after seeding. The number of multicellular (collective) projections around spheres was counted and calculated to the relative value to control U2OS cells.

Boyden chamber invasion assays

Stable RASSF1A expression was induced or not in U2OS and H1299 with 1 ug/ul doxycycline 24 hours before they were treated with 10 ng/ml TGFβ. NIH460 cells were transfected with FLAGRASSF1A and treated with 10 ng/ml TGFβ. HOP92 cells were treated with siRASSF1A (1) and treated with 10 ng/ml TGFβ. After 24 hours cells (1×10^5) were collected and cultured in the presence or not of TGFβ in the upper wells (in triplicates) of Transwell Matrigel Boyden chambers (BD Biosciences) and allowed to invade toward completed medium with 10% of FBS in the bottom wells. After 18 hours of incubation, invading cells were stained with 0.1% crystal violet, imaged, and manually counted using Adobe Photoshop software.

Plasmids:

FLAG-RASSF1A, HA-RASSF1A, Zsgreen-RASSF1A and MYC-RASSF1A plasmids were created by PCR. RASSF1A truncation mutants, mycRASSF1A 1-288, mycRASSF1A120-340, mycRASSF1A120-288 were created by PCR using mycRASSF1A as template. MYC-tagged Ub was previously described (Hamilton et al., 2014). FLAG-ITCH WT and FLAG-ITCH CA were kindly provided by Annie Angers, University of Montreal. TGFβRIHA and TGFβRI(TD)HA were kindly provided by Jeff Wrana, University of Toronto.

siRNAs:

RNA interference was performed using short interfering RNA (siRNA) oligonucleotides using Lipofectamin 2000 (Invitrogen). For silencing ITCH, SMAD2 and SMAD3 siGENOME Smartpool (GE Healthcare M-007196, M-003561, M-020067) were used. For silencing RASSF1A the oligos used were: GACCUCUGUGGCGACUU (siR1A1) or CACGUGGUGCGACCUCUGU (siR1A2). As control siRNA with the sequence UAAGGUAuGAAGAGAUAC designed to be non-targeting was used.

Antibodies:

The following antibodies were used in this study: RASSF1A (3F3, Santa Cruz), RASSF1A (eB114-10H1, e-bioscience), SMAD2 (Cell Signalling), pSMAD2 (Ser465/467) (Cell Signalling), SMAD3 (Cell Signalling), GAPDH (Cell Signalling), HA-tag (DW2, Millipore), HA-tag (Santa Cruz), FLAG-tag (M2, Sigma), MYC-tag (71D10, Cell Signalling), ITCH (Cell Signalling), YAP (H125, Santa Cruz), YAP (63.7 Santa Cruz), TAZ (V386, Cell Signalling), SMAD1 (Cell Signalling), pSMAD1 (Ser463/465) (Cell Signalling), p73 (Epitomics), TGF β RI (EP5124, abcam), TGF β RII (abcam), PUMA (abcam).

The sequences of primers used to detect target genes in qPCR were listed as below:

hSMAD7 forward: CCCATCACCTTAGCCGACTCTGC

hSMAD7 reverse: CCCAGGGGCCAGATAATTCGTTCC

hPAI-1 forward: ATTCAAGCAGCTATGGGATTCAA

hPAL-1 reverse: CTGGACGAAGATCGCGTCTG

hCTGF forward: CACCCGGGTTACCAATGACA

hCTGF reverse: GGATGCACTTTTGGCCTTCTTA

hGAPDH forward: AATCCCATCACCATCTTCCA

hGAPDH reverse: TGGACTCCACGACGTACTCA

h18S forward: AGTCCCTGCCCTTTGTACACA

h18S reverse: GATCCGAGGGCCTCACTAAC

mId1 forward : GAGTCTGAAGTCGGGACCAC

mId1 reverse: GATCGTCGGCTGGAACAC

m/d2 forward: ACAGAACCAGGCGTCCAG

m/d2 reverse: AGCTCAGAAGGGAATTCAGATG

m/d3 forward: CATAGACTACATCCTCGACCTTCA

m/d3 reverse: CACAAGTTCCGGAGTGAGC

mGapdh forward: CTCCACTCACGGCAAATTCA

mGapdh reverse: CGCTCCTGGAAGATGGTGAT

Supplementary References

Foty, R. (2011). A simple hanging drop cell culture protocol for generation of 3D spheroids. *Journal of visualized experiments : JoVE*.

Hamilton, G., Abraham, A.G., Morton, J., Sampson, O., Pefani, D.E., Khoronenkova, S., Grawenda, A., Papaspyropoulos, A., Jamieson, N., McKay, C., *et al.* (2014). AKT regulates NPM dependent ARF localization and p53mut stability in tumors. *Oncotarget* 5, 6142-6167.

Pefani, D.E., Latusek, R., Pires, I., Grawenda, A.M., Yee, K.S., Hamilton, G., van der Weyden, L., Esashi, F., Hammond, E.M., and O'Neill, E. (2014). RASSF1A-LATS1 signalling stabilizes replication forks by restricting CDK2-mediated phosphorylation of BRCA2. *Nat Cell Biol* 16, 962-971.

van der Weyden, L., Papaspyropoulos, A., Poulogiannis, G., Rust, A.G., Rashid, M., Adams, D.J., Arends, M.J., and O'Neill, E. (2012). Loss of RASSF1A synergizes with deregulated RUNX2 signaling in tumorigenesis. *Cancer Res* 72, 3817-3827.

Yee, K.S., Grochola, L., Hamilton, G., Grawenda, A., Bond, E.E., Taubert, H., Wurl, P., Bond, G.L., and O'Neill, E. (2012). A RASSF1A polymorphism restricts p53/p73 activation and associates with poor survival and accelerated age of onset of soft tissue sarcoma. *Cancer Res* 72, 2206-2217.